

**Yale University**  
**EliScholar – A Digital Platform for Scholarly Publishing at Yale**

---

Yale Medicine Thesis Digital Library

School of Medicine

---

January 2019

# The Role Of Traf3 And Cyld Mutationin The Etiology Of Human Papillomavirus Driven Head And Neck Cancers

Tejas Sudarshan Sathe

Follow this and additional works at: <https://elischolar.library.yale.edu/ymtdl>

---

## Recommended Citation

Sathe, Tejas Sudarshan, "The Role Of Traf3 And Cyld Mutationin The Etiology Of Human Papillomavirus Driven Head And Neck Cancers" (2019). *Yale Medicine Thesis Digital Library*. 3530.  
<https://elischolar.library.yale.edu/ymtdl/3530>

This Open Access Thesis is brought to you for free and open access by the School of Medicine at EliScholar – A Digital Platform for Scholarly Publishing at Yale. It has been accepted for inclusion in Yale Medicine Thesis Digital Library by an authorized administrator of EliScholar – A Digital Platform for Scholarly Publishing at Yale. For more information, please contact [elischolar@yale.edu](mailto:elischolar@yale.edu).

# The Role of TRAF<sub>3</sub> and CYLD Mutation in the Etiology of Human Papillomavirus Driven Head and Neck Cancers

A THESIS SUBMITTED TO THE  
YALE UNIVERSITY SCHOOL OF MEDICINE  
IN PARTIAL FULFILLMENT FOR THE  
DEGREE OF DOCTOR OF MEDICINE

TEJAS S. SATHE

ADVISORS: WENDELL G. YARBROUGH, MD, MMHC, FACS & NATALIA ISSAEVA, PhD

THESIS COMMITTEE MEMBERS: WENDELL G. YARBROUGH, MD, MMHC, FACS,  
NATALIA ISSAEVA, PhD, & KAREN ANDERSON, PhD

MAY 2019

© COPYRIGHT BY TEJAS S. SATHE, 2019. ALL RIGHTS RESERVED.

## ABSTRACT

The incidence of HPV-positive head and neck squamous cell carcinoma (HNSCC) continues to rise. Though HPV positivity is correlated with improved survival, up to a quarter of these tumors recur or metastasize despite aggressive therapy. Currently, there are no biomarkers that can identify HPV-positive HNSCC patients who would benefit from reduced doses of radiation—which when given at full dose carries significant morbidity. Through analysis of a limited cohort of The Cancer Genome Atlas (TCGA), we previously showed that two genes, TRAF3 and CYLD, were frequently deleted or mutated in HPV-positive HNSCC. TRAF3 and CYLD are functionally related negative regulators of the transcription factor NF- $\kappa$ B. In HNSCC, TRAF3 and CYLD mutations were correlated with increased NF- $\kappa$ B activity, the maintenance of HPV episomes, and improved patient survival. Thus, we hypothesize that a subset of HPV-positive HNSCC arises from a novel pathway of carcinogenesis dependent on dysregulation of NF- $\kappa$ B pathway intermediates such as TRAF3 or CYLD.

Survival analysis based on TRAF3/CYLD status was expanded to the entire TCGA HNSCC cohort. CYLD knockdown was achieved in vitro using CRISPR/Cas9. Western Blotting and a luciferase reporter assay were used to confirm CYLD depletion and NF- $\kappa$ B activation, respectively. Parental or CYLD-depleted cells were then transfected with HPV DNA and HPV replication was determined using qRT-PCR. Finally, long control region (LCR) transcriptional activity was assessed in parental or CYLD-depleted cells using a luciferase reporter assay as a correlate for HPV replication and gene expression.

We found that mutations in TRAF3 and CYLD accounted for 28% of HPV-positive HNSCC. Patients with HPV-positive tumors harboring TRAF3/CYLD mutations demonstrated markedly improved survival over patients with HPV-positive tumors without mutations or with HPV-negative tumors. CYLD knockdown in cultured cells resulted in constitutive activation of NF- $\kappa$ B in vitro. Preliminary data suggested that activation of NF- $\kappa$ B increased HPV replication and activity at the LCR.

Together, our data define a previously unrecognized subset of HPV-positive HNSCC that may rely on constitutively active NF- $\kappa$ B. Furthermore, mutations in TRAF3 and CYLD may serve as biomarkers in therapeutic de-escalation trials for HPV-positive HNSCC. Finally, we began establishing a cellular model that displays activation of NF- $\kappa$ B through CYLD depletion. This model will be useful to further investigate mechanisms of HPV-driven carcinogenesis in the head and neck.

# *Contents*

Abstract	iii
Introduction	I
Methods	20
Results	26
Discussion	40
References	52

## *Listing of figures*

1	Structure of the HPV virus and genome. . . . .	8
2	Classical Mechanism of HPV-driven carcinogenesis. . . . .	10
3	The Role of TRAF3 and CYLD in the NF- $\kappa$ B pathway. . . . .	14
4	TRAF3/CYLD genetic alterations in HPV-positive HNSCC, HPV-negative HNSCC, and cervical cancer. . . . .	28
5	TRAF3/CYLD Mutations in HPV-HNSCC. . . . .	29
6	Kaplan–Meier Survival Curves of HNSCC Patients in TCGA Cohort. . . . .	31
7	NF- $\kappa$ B Pathway Mutations in HPV-positive HNSCC in the Yale Cohort. . . . .	33
8	Immunoblotting of CYLD and phosphorylated p-65 in WT and CYLD deleted U2-OS cells. . . . .	34
9	NF- $\kappa$ B activity in CYLD-CRISPR clones and WT U2-OS cells. . . . .	36
10	HPV DNA at various time points in CYLD-CRISPR clones. . . . .	37
11	LCR Activity in CYLD-CRISPR Clones compared to WT U2-OS Cells. . . . .	39

TO MY LOVING FAMILY

## *Acknowledgments*

THIS THESIS IS THE RESULT of the hard work and guidance of many individuals. First and foremost, I would like to sincerely thank my mentor Dr. Wendell Yarbrough for inviting me to work in his laboratory. In Dr. Yarbrough, I was able to see the inspiring example of a surgeon-scientist, a path I hope to follow one day. I also would like to express my deepest gratitude to Dr. Natalia Issaeva, who ran the day to day workings of the laboratory and oversaw my project. Natalia helped me learn the methods required to perform the experiments for my project. When encountering hurdles, she patiently guided me in troubleshooting protocols and provided workarounds when necessary. She allowed me to better understand the practical techniques required to successfully complete experiments as well as the scientific principles behind them. Her mentorship increased my work ethic and my knowledge of the science. I can say she taught me the importance of scientific integrity and performing high quality work, characteristics I hope to carry on as a scientist in my own right. Finally, this work would not have been possible without my friends and family. My brother Ojas, my mother Swati and my father Sudarshan have supported me through every endeavor, especially medical school and this thesis. To my Yale family—the friends and mentors that have guided me over the past five years, thank you for everything!



# *Introduction*

## **Cancers of the Head and Neck**

Cancers of the head and neck can affect the ability to swallow, speak, taste, hear, and even breathe. In short, they can impact many of the senses that help us interact with the world around us. Cancer, in any organ, at any stage, is a fearsome entity, but in the precious real-estate of the head and neck anatomy, even small tumors can wreak havoc on the normalcy of life. The majority of these tumors are classified as Head and Neck Squamous Cell Carcinoma (HNSCC), a description that indicates both their anatomic and cellular origin. These cancers arise from cells of the epithelial surfaces that line the organs and cavities of the aerodigestive track.<sup>1</sup>

The early clinical manifestations of HNSCC can be minimal or vague, highlighting the advanced stages of disease at which most patients are diagnosed. HNSCC can cause non-healing or painful ulcers, difficulty or painful swallowing (dysphagia or odynophagia, respectively), hoarseness of voice, difficulty breathing, headaches, ear pain (otalgia), and problems hearing—including a ringing sensation of the ears (tinnitus). Friable tumors may bleed from the nose or mouth, leading to additional symptoms, and as with all cancers, systemic symptoms such as weight loss, fevers, and fatigue may occur. Lumps or masses may arise either from the primary tumor or any involved cervical lymph nodes, and although these are not usually painful, they are usually noticed by the patient, family member, or care provider due to their mass effect.<sup>2</sup> The current standard of treatment for HNSCC in-

cludes combinations of surgical resection, cervical lymphadenectomy, chemotherapy, and high dose radiation (i.e. 70 Gy). Following resection, a functional and cosmetic reconstruction is attempted if necessary and technically feasible.<sup>2</sup>

While the morbidity of this disease is clear, the morbidity associated with treatment is not to be overlooked. Radiation, in particular, is associated with side-effects including difficulty chewing, eating, or swallowing food, changes in speech, increased tooth decay, difficulty with dentures, and fibrosis of the muscles of the neck. According to a recent quality of life study by Epstein and colleagues, over half of the respondents reported pain, problems with mood, and interference of social activity. Almost all respondents reported having dry mouth.<sup>3</sup> For patients with advanced disease, one in two affected individuals die within five years, a 50% mortality that persists despite the best available therapies currently available. Thus, there remains a clear need not only for more effective but also more discriminating therapies that reduce both cancer and radiation related morbidity.<sup>1</sup>

### The Etiology of HNSCC

HNSCC has a multifactorial etiology. The majority of HNSCC is associated with tobacco exposure with a synergistic risk for patients who concomitantly use ethanol.<sup>1,2</sup> Cancer arises after mucosal exposure to these factors with frequent development of field cancerization, the widespread mutation and DNA damage of swaths of exposed tissue. In fact, a high degree of mutation in the essential tumor suppressor p53 is observed.<sup>2</sup> Recently, a subset of HNSCCs was found to be associated with infection by the human papillomavirus (HPV). A landmark study by Kari Syrjanen and colleagues demonstrated that biopsies of some oropharyngeal squamous cell carcinomas morphologically and immunohistochemically resembled HPV lesions.<sup>4</sup> Since then, the clinical relationship between HPV infection and HNSCC has been more intensely studied, yet the mechanisms by which HPV causes cancer in the head and neck remain poorly understood.

## The Role of HPV in HNSCC

The majority of HPV-positive HNSCC arise from the oropharynx.<sup>5</sup> In fact, recent estimates suggest that greater than 70% of oropharyngeal squamous cell carcinomas in the U.S. are attributable to HPV.<sup>6,7,8,9</sup> HPV infection was previously known to cause cervical cancer, and the discovery of a novel tumor type associated with this virus has challenged existing assumptions about virally-driven oncogenesis. Similar to cervical cancer, HPV-positive HNSCC is thought to be sexually transmitted, but unlike uterine cervical carcinoma, the incidence of HPV-positive HNSCC is on the rise and the trend of rising incidence will likely continue. Notably, this rise is seen predominantly among non-smokers in the developed world.<sup>5</sup> Currently, more individuals in the U.S. are diagnosed with HPV-associated HNSCC compared to cervical cancer. Thus, HNSCC, and especially the HPV-positive subtype, represent an emerging public health concern.<sup>1</sup>

While both HPV-positive and HPV-negative tumors affect the same cells and cause a similar symptom profile, there are a number of important differences that highlight the divergent natures of these two diseases. Anatomically, HPV-positive tumors tend to originate in the oropharynx, as opposed to HPV-negative tumors which have diverse origins throughout the upper aerodigestive track. Epidemiologically, HPV-positive HNSCC patients tend to be younger, more educated, have higher socioeconomic status, and less exposure to tobacco and alcohol.<sup>10</sup> Perhaps most interestingly, HPV-positive tumors are associated with improved survival, compared to stage matched HNSCC that is HPV negative. A prospective trial by the Eastern Cooperative Oncology Group showed that HPV status correlated with improved responsiveness to induction chemotherapy and chemoradiation and improved survival, both overall and adjusted for patient and tumor characteristics.<sup>11</sup> This would suggest that HPV-status alone could be utilized to guide treatment plans. Currently, this is not the case, likely because 25% of HPV-positive patients have aggressive disease that leads to recurrence and metastasis despite current available therapies.<sup>12</sup>

While there are clear clinical dissimilarities between HPV-positive and HPV-negative

HNSCC, novel genomic technologies are elucidating differences at the molecular level between these two tumor types. The Cancer Genome Atlas (TCGA) embarked on a genomic analysis of over 500 HNSCCs to analyze the mutational landscape of this disease.<sup>5</sup> One surprising finding from this landmark study was that the TNF receptor-associated factor 3 (TRAF3) gene was inactivated in roughly a quarter of HPV-positive tumors, either by deletion (14%) or truncation (8%). TRAF3 is an immune modulator that plays roles in innate and adaptive immunity. Specifically, TRAF3 is known to be a critical component of interferon type 1 signaling in response to viral infections.<sup>13</sup> While this deletion has been observed in multiple myeloma and nasopharyngeal carcinoma, it has not been previously described in HPV-associated cancers.<sup>14,15,16</sup> On the other hand, mutations in TP53 are observed in the overwhelming majority of HPV-negative HNSCC, but rarely seen in the HPV-positive variant.<sup>5</sup> In addition to these differences, further studies have elucidated that HPV-positive and HPV-negative HNSCC have distinct genomic, proteomic, and epigenetic profiles.<sup>17,18,19</sup>

### HPV-positive HNSCC and Cervical Cancer

While it is clearly accepted that HPV-positive and HPV-negative HNSCC are distinct clinical entities, a number of differences suggest that HPV-positive HNSCC may be distinct from HPV-driven cervical cancer as well, and these differences can be a template for understanding biological variability between HPV-driven cancers.

First, HPV16 and HPV18 account for 70% of cervical cancer, with other high-risk subtypes accounting for the remainder. In contrast, HPV16 alone causes over 90% of HPV-positive HNSCC.<sup>20,21</sup> Second, Parfenov and colleagues performed a genomic analysis of 35 HPV-positive HNSCC and found that 10 genomes (29%) did not demonstrate HPV integration. Moreover, among genomes with integrated HPV, a number did not show increased expression of the oncoproteins E6 and E7.<sup>18</sup> Both HPV genome integration and increased E6 and E7 expression were thought to be critical to HPV-driven carcinogenesis

in cervical cancer. The fact that a notable minority of HPV-positive HNSCCs lack these features lends credence to an alternative mechanism of HPV carcinogenesis that may be active in the head and neck.

An urgent need for improved screening and therapy for HNSCC is needed to detect earlier stages of disease and provide more effective therapeutic interventions. However, among patients who respond well to treatment, the morbidity of radiation can often cause an additional expense to quality of life. This problem is highlighted predominantly in the HPV-positive cohort because of their longer life expectancy and higher cure rates. To decrease morbidity related to therapy, investigators have posed the question of whether lower doses of radiation may provide an equivalent oncologic outcome while saving patients from treatment-associated morbidity. The minority of HPV-positive patients with aggressive disease precludes using HPV status exclusively as a marker to identify those patients suitable for therapeutic de-escalation. Current clinical trials such as ECOG 1308 select for deintensified therapy based on patient response to induction therapy, but there are currently no established biomarkers that can select patients for de-escalation prior to treatment. This remains an important goal of head and neck oncology. Furthermore, in addition to driving changes in patient care, characterizing novel mechanisms of HPV-driven carcinogenesis represents a new era in understanding HPV biology.

In the following sections, we briefly review the salient elements of HPV and HNSCC biology that pertain to our work as well as the preliminary work our laboratory has performed in elucidating novel mechanisms of HPV-driven carcinogenesis in the head and neck.

### **The Biology of HPV**

The history of understanding HPV and its role in cancer traverses centuries as well as countries. In 1842, the Italian physician Rigoni-Stern first posited a sexually transmitted etiology for cervical cancer upon observing a paucity of cases among women who were

not sexually active.<sup>22,23</sup> However, at that time little was known about infectious diseases or the organisms that cause them. The term condyloma dates to the time of Hippocrates. While the ancient Greeks and Romans believed that genital warts were infectious. Ciuffo proved that the causative agent was a virus by inoculating skin using the extract of warts passed through sufficiently small filters. A similar association between laryngeal warts and the same infectious agent was later demonstrated. Only in 1949 did Strauss and colleagues visualize the virus using electron microscopy<sup>22,24,25</sup>

In the twentieth century, the idea that a virus could cause cancer was also taking hold. A series of quixotic experiments on chicken sarcomas first intrigued the American scientist Peyton Rous on this possibility. While he was widely discredited by his contemporaries, his work laid the foundation for Rous and colleagues to determine a carcinogenic effect of rabbit papillomaviruses.<sup>22,26,27,28</sup> Over the next few decades, that variability and diversity of papillomaviruses became clear. Perhaps the most significant discovery was by the German Scientist Harald zur Hausen, who isolated HPV DNA from cervical tumor specimens.<sup>29,30,31,22</sup> While the subtype of HPV (type 16) that causes the vast majority of HN-SCC are covered by existing vaccines, whether these vaccines prevent HNSCC has not yet been studied.

Human papillomavirus (HPV) is a virus that is characterized by a circular, 8 kb genome consisting of dsDNA surrounded by an icosahedral capsid lacking a membranous envelope. HPV has a proclivity for cells of the cutaneous and mucosal epithelia, and as a result, HPV infections can manifest in the oral, urogenital, and anogenital tracts as well as the skin surrounding these areas. HPV is the most common sexually transmitted infection, with over two-thirds of sexually active adults exposed to HPV DNA in the first two years of sexual activity. HPV viruses are thought to enter the skin or mucosa through micro-abrasions where they infect cells of the basal epithelia. While the majority of individuals affected may experience subclinical disease, the most common clinical manifestation is warts, or condyloma acuminatum. Risk factors for HPV infection include multiple sexual partners,

oral contraceptive use, pregnancy, and disruption of the normal immune response. While lesions can last from 12–18 months, they mostly represent benign proliferations of epithelial cells. While the absolute risk of progression to malignancy is low, HPV still accounts for a significant oncologic morbidity through its causal association with cervical cancer where 470,000 women are diagnosed worldwide. At this point, it is believed that virtually all cervical cancer is caused by HPV infection. While there are over 100 types of HPV described, the majority of cancers arise from high-risk types 16, 18, 31, 33, 45 and 51. The development of prophylactic vaccines against high-risk HPV subtypes holds the promise of eventually eradicating HPV and cervical cancer. However, lack of access to vaccination combined with incomplete vaccine coverage in the developing world suggests that HPV infection and progression to cervical cancer will continue to be an area of public health concern for decades to come.<sup>32,33</sup> While the subtypes of HPV that cause HNSCC are covered by existing vaccines, whether these vaccines prevent HNSCC has not yet been studied.<sup>34</sup>

Most of our understanding of HPV biology and oncogenesis derives from the experience with cervical cancer. The HPV genome consists of eight open reading frames (ORFs) that are transcribed as polycistronic mRNAs. The HPV life cycle can be divided into two stages—early and late, each with a respective promoter that drives expression of proteins needed in that stage. One structural element, the long control region (LCR) regulates transcription of early genes. The early genes, E1, E2, E4, E5, E6, and E7 are primarily involved with HPV replication, pathogenesis, and oncogenesis. The late genes, L1 and L2, are involved with the assembly of new virions and the spread of infection ??.<sup>32,35</sup>

The main role of the viral E1 protein is in genome replication. E1 binds to HPV DNA, helps unwind it, and drives recruitment of polymerase machinery to the viral genome. The HPV E2 protein has a dual role in facilitating replication and transcription, and E2 potentiates E1 binding to viral DNA. E2 also binds to multiple sites in the LCR, where it promotes viral gene expression at low concentrations but represses expression at high con-

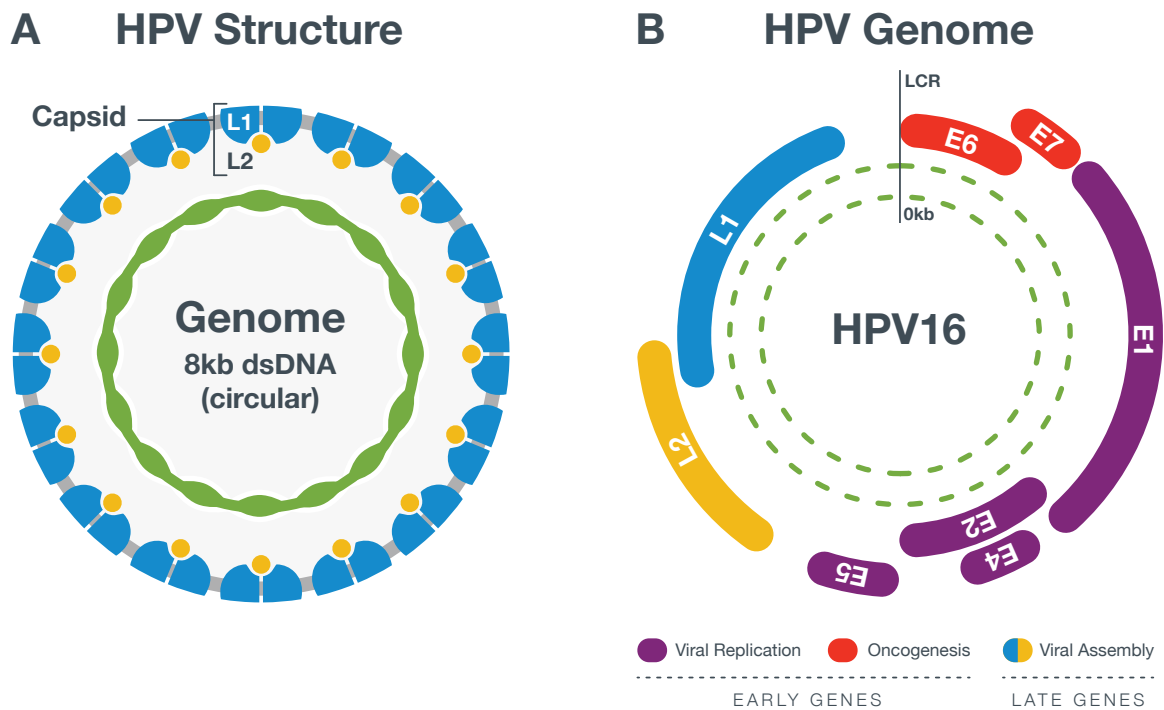


**Figure 1.** Structure of the HPV virus and genome. (A) HPV is a non-enveloped double-stranded DNA virus. The circular, 8kb genome is surrounded by a capsid consisting of the major capsid protein L1 and the minor capsid protein L2. L1 and L2 form complexes that arrange into an icosahedral confirmation during viral assembly. (B) The HPV genome contains both early genes involved in viral replication and oncogenesis and late genes coding for a viral capsid.



centrations. Furthermore, E2 is thought to aid in episomal maintenance and tether HPV DNA to replicating chromosomes, ensuring that viral genes are delivered to daughter cells during cell division. The function of E4 and E5 is less well understood. E4, commonly expressed as an E1E4 splice variant, is a highly expressed HPV protein that may play a role in viral replication or exit of mature virions in the later part of the HPV life cycle. E5 is a small protein that is thought to augment the oncogenic activity of E6 and E7.<sup>32</sup>

E6 and E7 are the viral proteins that drive malignant transformation. The currently understood mechanism of HPV-driven carcinogenesis comes from study of these two oncoproteins. E6 and E7 function by disabling the major tumor suppressors in human cells. E6 complexes with the host protein E6AP and binds p53, marking it for proteasomal degradation. E7 directly binds and similarly targets the tumor suppressor Rb for proteasomal degradation. Through a multitude of downstream effectors, p53 and Rb protect the cell from oncogenic transformation by halting progression and activating apoptosis. Thus, HPV acts by releasing the brakes on cell-cycle regulatory pathways, thereby promoting unregulated DNA replication and mitosis. At baseline, E2 expression inhibits active transcription of the E6 and E7 genes. Interruption of the E2 reading frame by viral integration into the host genome reverses this inhibition and is thought to be a critical step in virally-mediated oncogenesis. Interestingly, via inhibition of Rb, E7 also increases expression of p16, a tumor suppressor that in the presence of Rb is responsible for G1/S arrest. For this reason, p16 is considered a highly reliable marker for HPV-positive HNSCC, and current AJCC guidelines call for the use of p16 in the identification of HPV-positive tumors.<sup>2, 32,36</sup>

The late HPV proteins, L1 and L2, form an icosahedral capsid around HPV genomes in order to produce mature virions. They are only expressed in terminally differentiated epithelial cells that are closer to the skin or mucosal surface. This pattern of expression is thought to be due to the high immunogenicity of L1 and L2 and the relative dearth of immune surveillance farther away from the basal layers. The L1 protein is the basis for HPV vaccines currently in use.<sup>32</sup>

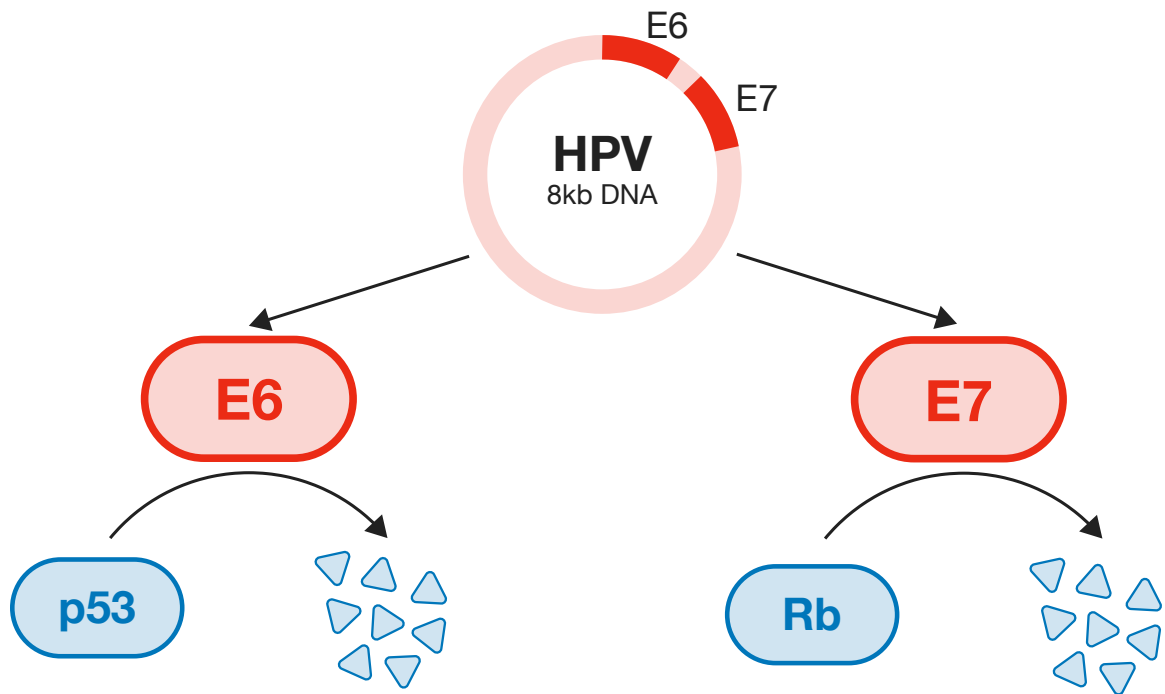


**Figure 2. Classical Mechanism of HPV-driven carcinogenesis.** Much of the current understanding of HPV-driven carcinogenesis comes from the study of cervical cancer. In this tumor type, the oncoproteins E6 and E7 lead to the degradation of the tumor suppressors p53 and Rb, respectively. One role of p53 and Rb is to arrest the cell cycle at G1/S checkpoint and to activate apoptosis, so removal of these proteins leads to uncontrolled cell division. The seminal event that leads to initiation of the oncogenic pathway is viral integration into the host genome which allows E6 and E7 expression to commence.

By changing the expression levels of these proteins at different points in the HPV life cycle, HPV is able to efficiently invade and establish infection in the actively differentiating tissue of the epithelium. Basal cells of the epithelium actively divide, leaving a population of stem cells from which to regenerate the epithelium as well as a population of cells that migrate upwards and cease mitotic activity. Throughout this migration, cells produce additional amounts of keratin, terminally differentiate, and eventually die. By exploiting micro-abrasions in skin or mucosal surfaces, HPV evade the traditional barriers these surfaces provide and infect cells of the basal layers. In these undifferentiated cells, the early program of HPV maintains replication at a low copy number. As cells migrate and differentiate, they transition to the late program, characterized by high copy numbers of the HPV genome, production of capsid, viral assembly, and egress of mature virions, which allows the process to repeat.<sup>32</sup>

During the normal infectious cycle, high expression of E2 limits activity of E6 and E7. However, persistent infection by HPV increases the chances of viral integration, during which the E2 gene is frequently disrupted, disinhibiting E6 and E7 expression. As previously described, this promotes cellular progression through the G1/S checkpoint and persistent replication. Together with other events that are not well understood, overexpression of E6/E7 triggers a transformative pathway of increased dysplasia leading ultimately to complete malignant transformation. On a diagnostic pap smear, this is characterized as progression of Cervical Intra-epithelial Neoplasia (graded 1 to 3) to outright cancer.<sup>32</sup>

### **Nuclear Factor- $\kappa$ B**

The finding that TRAF3 was preferentially inactivated in HPV-positive HNSCC suggested a role for NF- $\kappa$ B in HPV-driven carcinogenesis. Here, we briefly describe the NF- $\kappa$ B pathway, the role of ubiquitin in the regulation of this pathway, and the importance of TRAF3 and other proteins in that regulatory landscape.

Nuclear factor-kappa-B (NF- $\kappa$ B) is a complex transcription factor with many down-

stream effects. In particular, it can be thought of as the quarterback of the inflammatory response, directing a multitude of downstream factors to promote inflammation and protect the cell from infectious insults. Moreover, NF- $\kappa$ B has also been implicated in driving cellular changes that promote transformation into cancer through activation of diverse signaling pathways and protection from cell death.

NF- $\kappa$ B was discovered fortuitously by Ranjan Sen and David Baltimore in 1986, who found that a nuclear protein bound to the enhancer region of the immunoglobulin kappa-light chain of B-cells, leading to the synthesis of immunoglobulin light chains.<sup>37</sup> While discovery of this factor marked momentous turning point in cell biology, it was the subsequent discoveries by this group that were even more profound. First, they found that NF- $\kappa$ B was not restricted to B-cells but rather ubiquitously observed in all cells, hinting at an ancient and conserved origin for this protein.<sup>38</sup> Second, a series of experiments by Patrick Baeuerle and Baltimore led to the discovery that DNA binding by NF- $\kappa$ B following stimulation with lipopolysaccharide (LPS) did not require "de novo protein synthesis", hinting that this factor was present but inactive under normal conditions. When NF- $\kappa$ B binding of DNA was shown to increase following the application of translational inhibitors, it was hypothesized that the agent responsible for inactivating NF- $\kappa$ B was transient. In 1988, the family of agents responsible was identified and named inhibitor of kappa-b (I $\kappa$ B).<sup>39</sup>

A Nature review commemorating 25 years since the discovery of NF- $\kappa$ B stated that over 35,000 articles have been written about NF- $\kappa$ B and its biology, signaling pathways, and effects of the immune system, response to infection, and cell survival. Here, we present a brief overview of NF- $\kappa$ B as it relates to our work in head and neck cancer.<sup>38</sup> While it was clear that NF- $\kappa$ B was broadly consequential to immunology, the discovery that one NF- $\kappa$ B subunit called p50 had homology to the avian oncoprotein v-Rel presaged NF- $\kappa$ B's relevance in pathways of carcinogenesis as well.<sup>39</sup>

Today, we understand that the transcription factor NF- $\kappa$ B is actually a family of five related proteins that share the Rel domain, which is responsible for dimerization and DNA

binding. These proteins are: p65 (RelA), c-Rel, RelB, p105 and p100. p105 and p100 are precursor proteins that are degraded to p50 and p52, respectively. Prior to activation and DNA binding, these subunits dimerize. The most common combinations are p50-p65 (RelA) and p52-RelB. Activation of NF- $\kappa$ B to the point where these two heterodimers can bind DNA and execute their downstream effects is the result of two respective, tightly-regulated pathways.<sup>40</sup>

In both pathways, the penultimate step to activation is release of the NF- $\kappa$ B heterodimers by the inhibitory factor I $\kappa$ B. Cytoplasmic sequestration of NF $\kappa$ B by I $\kappa$ B is overcome when I $\kappa$ B is phosphorylated by I $\kappa$ B Kinase or IKK. IKK itself is a family of proteins: two catalytically active subunits IKK $\alpha$  and IKK $\beta$  and a regulatory subunit IKK $\gamma$  (also called NEMO). The phosphorylation of NEMO regulates whether IKK is active and able to phosphorylate I $\kappa$ B.<sup>40</sup>

The canonical pathway is more commonly activated by physiologic stimuli. In this pathway, cytokine signals from receptors such as tumor necrosis factor receptor (TNFR) and interleukin 1 (IL-1) receptor (IL-1R), as well as markers of infection such as Toll-like receptor 4 (TLR4) lead IKK $\beta$  and NEMO to phosphorylate I $\kappa$ B and lead to the translocation of p50-p65 heterodimers into the nucleus. Conversely, the non-canonical pathway is primarily activated by factors such as CD40 ligand, BAFF, and lymphotoxin- $\beta$ 2. In this pathway, IKK $\alpha$  phosphorylation mediates processing of p100-RelB complexes into p52-RelB complexes which are active and can translocate into the nucleus. This degradative processing is activated by NF- $\kappa$ B inducing kinase (NIK). At baseline, the p100 subunit plays an inhibitory role until it is processed into p52. Interestingly, while canonical activation of NF- $\kappa$ B is rapid, non-canonical signaling is slower and occurs on the order of hours.<sup>41</sup>

Given the highly conserved nature of this regulatory pathway, most regulation and modification to NF- $\kappa$ B biology is seen between the initial receptor-mediated signaling that occurs at the cell membrane and the activation of the IKK complex. This regulation relies

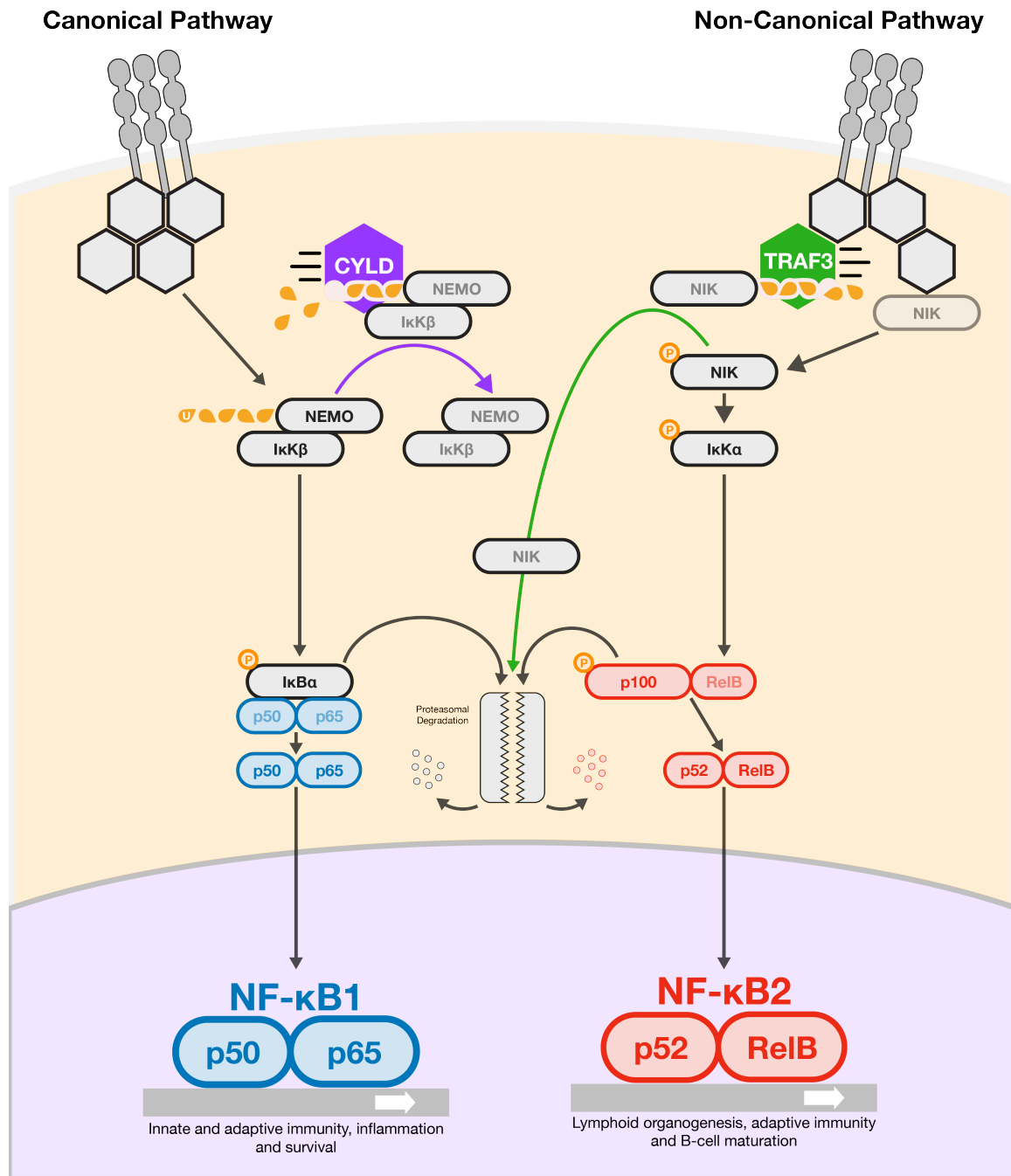


**Figure 3.** The Role of TRAF3 and CYLD in the NF- $\kappa$ B pathway. TRAF3 is an E3 ubiquitin ligase that adds ubiquitin moieties to NIK, marking it for proteasomal degradation. Once degraded, NIK can no longer activate IκKα, which activates NF- $\kappa$ B in the non-canonical pathway. CYLD is a deubiquitinating enzyme that removes ubiquitin moieties from NEMO, the regulatory subunit of IKK. By doing so, it prevents IKK from phosphorylating IκB and releasing active NF- $\kappa$ B in the canonical pathway. In this figure, IKKα, IKKβ, and NEMO are shown separately for simplicity. In reality, these three proteins form the IKK complex. Thus, TRAF3 and CYLD serve as negative regulators of NF- $\kappa$ B signaling. Absence or inactivation of either of these two proteins leads to constitutive activation of NF- $\kappa$ B. While CYLD primarily acts in the canonical pathway and TRAF3 primarily acts in the non-canonical pathway, significant crosstalk between the two pathways suggests that this demarcation may not be absolute.

heavily on ubiquitin-dependent signaling.

The ubiquitin system is responsible for the degradation of proteins, allowing for the recycling of amino acids for other biochemical processes and regulating the turnover of proteins whose expression is required transiently. Ubiquitin itself is a protein of modest size comprising of only 76 amino acids. Ubiquitin is added to proteins as a molecular tag via a three-step pathway. First, ubiquitin is activated by the protein E1. Second, the carrier protein E2 binds ubiquitin. Finally, an E3 ubiquitin ligase binds the protein of interest and catalyzes the addition of ubiquitin to a Lysine residue of that protein. The rich diversity of E3 ubiquitin ligases and their specificity towards specific substrate proteins allows for precise targeting and regulation in the ubiquitin pathway.<sup>42,43</sup> This process is repetitive and results in the synthesis of poly-ubiquitin chains on proteins. In addition, there are times when removal of ubiquitin is required for appropriate signaling. For this purpose, proteins called deubiquitinases catalyze the hydrolysis of ubiquitin from a poly-chain.<sup>43</sup>

Ubiquitination typically occurs on lysine residues, either on the substrate proteins or on other ubiquitin proteins themselves in order to form chains. The nature of this lysine bond, however, can drive the ultimate fate of ubiquitin-mediated signaling. Ubiquitin itself has seven lysine residues, of which the most commonly used are K48 and K63. K48 linked poly-ubiquitin tails mark proteins for degradation by the 26S proteasome. In NF- $\kappa$ B signaling, I $\kappa$ B is degraded by a K48-linked poly-ubiquitination mechanism. On the other hand, K63 linked poly-ubiquitin tails play a role in non-proteolytic signaling. Deubiquinating enzymes (DUB) play an especially important role in the latter type of signaling.<sup>42,43,44</sup>

Among the proteins that utilize ubiquitin to drive downstream signaling, the TNFR-associated factor (TRAF) family of proteins appears to play a critical role. TRAFs assemble into protein complexes on the intracellular surface of membranes where they can relay signals from membrane receptors to downstream effectors.<sup>40</sup> In this role, they are responsible for regulating signaling in various immunologic, inflammatory, and cell survival pathways

as well as crosstalk between pathways. In total, seven TRAF proteins (TRAF1-7) have been described. All of them share a TRAF domain that facilitates binding to surface receptors and creating protein complexes that enable downstream signaling. Interestingly, all except TRAF1 appear to have E3 ubiquitin ligase capability, highlighting both their structural and functional role in pathway regulation.<sup>40</sup> In canonical NF- $\kappa$ B signaling, TRAF2 associates with two E3 ubiquitin ligases called central Inhibitor of Apoptosis (cIAP) 1 and 2 as well as the kinase RIP1. K63-linked polyubiquitination of RIP1 by cIAP1 and cIAP2 leads to activation of IKK and activation of NF- $\kappa$ B signaling. In the non-canonical pathway, TRAF3, an E3 ubiquitin ligase, drives polyubiquitination of NIK and leads to its degradation, preventing processing of p100-Rel by IKK $\alpha$ . Thus, TRAF3 exhibits an inhibitory effect on NF- $\kappa$ B signaling. Interestingly, TRAF2 and cIAP2 also degrade TRAF3 so that TRAF3 depletion and subsequent NF- $\kappa$ B signaling is transient.<sup>40,45,46</sup> This is one example of cross-talk between the canonical and non-canonical pathways.<sup>40</sup> NIK and non-canonical NF- $\kappa$ B activity was shown to be elevated in multiple myeloma, the result of NIK amplification or deletion of TRAF2, TRAF3, cIAP1, and cIAP2.<sup>45,16</sup>

While the role of E3 ubiquitin ligases in NF- $\kappa$ B mediated signaling has been clearly established, the discovery of CYLD as a deubiquitinating enzyme heralded the discovery that removing ubiquitin from proteins was also a key part of this pathway. Located on chromosome 16, the Cylindromatosis (CYLD) gene encodes a 956 amino acid protein including a C-terminal domain that is highly conserved among deubiquitinating enzymes. CYLD is a tumor suppressor gene that was found to be mutated in familial cylindromatosis, a condition marked by numerous benign tumors of the skin appendages; however, its function remained unclear until its discovery as a deubiquitinating enzyme.<sup>47,48,49</sup>

Brummelkamp and colleagues identified 50 candidate deubiquitinating genes containing the aforementioned C-terminal domain common to all deubiquitinases. They generated small-hairpin RNAs against each of these candidate genes to knock-down expression and then tested NF- $\kappa$ B activity in U2-OS cells using a luciferase reporter assay. The only



gene that was found to be associated with NF- $\kappa$ B activation was CYLD.<sup>50</sup> Subsequent molecular studies identified that CYLD bound to NEMO, TRAF2, and TRAF6. CYLD is thought to hydrolyze K63-linked ubiquitin chains on target proteins. In canonical NF- $\kappa$ B signaling, deubiquitination of NEMO prevents it from activating I $\kappa$ B, thereby abrogating activation and translocation of p52-p60.<sup>48,49</sup> CYLD association with TRAF2 and TRAF6 also suggest a role in the non-canonical pathway. In fact, CYLD deletions were also associated with multiple myeloma in the previously mentioned study.<sup>16</sup>

In summary, TRAF3 inhibits NF- $\kappa$ B signaling through the non-canonical pathway while CYLD inhibits NF- $\kappa$ B signaling through the canonical pathway. However, due to cross-talk between both pathways, some crossover in this mechanism is not precluded. Overall, inactivating mutations in TRAF3 or CYLD disinhibits NF- $\kappa$ B signaling, resulting in constitutive translocation of active NF- $\kappa$ B into the nucleus and persistent expression of NF- $\kappa$ B induced gene.

### Previous Work

While TRAF3, CYLD, and other genes of this pathway had known functions in NF- $\kappa$ B signaling and had been implicated in various hematologic malignancies, their role in solid tumorigenesis was not previously described. This paradigm dramatically changed when The Cancer Genome Atlas sequenced both HPV-positive and HPV-negative tumors. Recent work by our laboratory has shed new light on TRAF3 and CYLD, highlighting their possible involvement in HPV-driven carcinogenesis of the head and neck. As previously mentioned, the majority of HPV-positive HNSCC respond better to therapy with improved survival compared to HPV-negative tumors. However, because about 25% of these tumors will recur, there is a clinical need to classify HPV-positive tumors to identify those with good and poor survival. We recently reported data from The Cancer Genome Atlas that suggest that TRAF3 and CYLD mutations correlate with survival benefit in HPV-positive HNSCC.<sup>12,5,18</sup>

The Cancer Genome Atlas showed that TRAF3 was preferentially mutated in HPV-positive HNSCC (n=35). Our laboratory performed an in-depth analysis of TCGA data and discovered that among the HPV-positive HNSCC studied, 25% had mutations in TRAF3. 55% of these mutations were deletions while the remainder were truncations suggesting that loss of TRAF3 function was required in these tumors. TRAF3 was mutated in 2.5% of HPV-negative HNSCC and 4% of cervical cancers. However, in both cases, these mutations were equally divided between deletions and amplifications. We also showed that CYLD was preferentially mutated in 11% of HPV-positive HNSCC (n=35), with identification of both truncations and deleterious missense mutations. CYLD was mutated in only 2.9% of HPV-negative HNSCC and in 2% of cervical cancers. In HPV-negative HNSCC, amplifications of CYLD were also observed. The functional relationship between TRAF3 and CYLD in NF- $\kappa$ B pathway regulations makes these observations mechanistically cohesive. In all, these data demonstrate that 36% of HPV-positive HNSCC contain inactivating mutations in TRAF3 or CYLD. Further analysis based on gene expression suggested that HPV+ tumors with TRAF3 or CYLD defects had increased NF- $\kappa$ B activity compared to cancers lacking TRAF3 or CYLD mutations. While NF- $\kappa$ B overactivation is a hallmark feature of many tumor types, it has not been previously described in HNSCC.<sup>51</sup>

Identification of these mutations opened a line of investigation into whether they endowed their tumors with unique biologic or clinical features. In addition to increased NF- $\kappa$ B activity, TRAF3 or CYLD mutations also correlated with lack of HPV genome integration. The most dramatic result of this study was that TRAF3/CYLD mutations correlated with improved survival when compared to either HPV-positive HNSCC without these mutations and HPV- negative HNSCC.<sup>12</sup>

These data not only demonstrate that TRAF3/CYLD mutations characterize a unique subset of HPV-positive HNSCC, but also support the hypothesis that TRAF3/CYLD mutation is responsible for improved survival in HPV-positive HNSCC. Furthermore, these data suggest that in HPV-positive HNSCC with TRAF3/CYLD mutations, cancer is

arising via a previously unknown mechanism that is based on the overactivation of NF- $\kappa$ B and episomal HPV. These data present us with the task of characterizing the role of TRAF3/CYLD inactivation in HPV-driven HNSCC both biologically, through the construction of in vitro models, and clinically, through the development of prospective trials.

The aim of our work is to characterize how these mutations create a favorable landscape for HPV infection and subsequent progression to head and neck cancer. Furthermore, we hope to elucidate whether these mutations can be used as reliable biomarkers to predict which HPV-positive HNSCC patients could benefit from lower doses of radiation.

# *Methods*

THE METHODS USED in this study include culture of cell lines, CRISPR/Cas9 gene knock-out, immunoblotting, quantitative real-time polymerase chain reaction (qRT-PCR), the purification of DNA and RNA, and the use of luciferase reporter assays. The details of these methods are described in the following section and were performed by this author with guidance from Natalia Issaeva and Cassie Pan. In addition, genetic mutation analysis through cBioportal and gene set enrichment analysis was performed by Dr. Michael Hajeck, Dr. Andrew Sewell, Dr. Natalia Issaeva, and Dr. Wendell Yarbrough. Generation of Kaplan-Meier survival curves was performed by Dr. Natalia Issaeva. Overall study design was guided by Dr. Natalia Issaeva and Dr. Wendell Yarbrough.

## **Survival Analysis of Expanded TCGA Cohort**

Data regarding TRAF3 and CYLD mutations in both HPV-positive and HPV-negative HNSCC were obtained from cBioPortal for Cancer Genomics (available at: [www.cbioportal.org](http://www.cbioportal.org)). Schematic figures were downloaded and adapted from the portal. A dataset containing survival information for HNSCC patients was obtained from a prior study (reference). Kaplan-Meier survival curves were produced using GraphPad Prism 7 software, and the log-rank (Mantel-Cox) test was used for statistical analyses.

### Analysis of Yale HNSCC Cohort

HPV-positive tumors were obtained from the Yale HNSCC biorepository cohort. Genomic DNA was purified from tumor samples, with matched blood used as a control. Using the ten NF- $\kappa$ B pathway genes that were altered in the HNSCC cohort of TCGA as a reference, targeted sequencing was performed on tumor samples. Demographic information, smoking status, clinical characteristics of tumors, status of recurrent disease, and finally survival information were obtained from the Yale electronic medical record. HPV-positivity was confirmed by either documented HPV PCR or p16 testing.

### Construction of Circular HPV DNA

Bacterial plasmids consisting of intact HPV16 genomes incorporated into the pBluescript SK plasmid vector containing an ampicillin resistance marker (ATCC 45113DTM) were transformed into competent *E. coli* and plated on LB containing ampicillin. Resultant colonies were expanded overnight in LB cultures and pelleted. DNA was extracted using QIAprep Spin Miniprep Kit (Qiagen) according to the manufacturer's protocol. DNA was then sequentially digested with BamHI and BglII (New England Biolabs). To re-circularize the linear fragments, DNA ligation was performed with DNA ligase I overnight at 37 degrees Celsius. Following each digestion and ligation, DNA was collected using Monarch® PCR & DNA Cleanup Kit (New England Biolabs), according to the manufacturers protocol to remove protein from the sample. Synthesis was confirmed by resolving DNA on a 1% agarose gel and SYBR Safe dye and observing an 8kb band consistent with circular HPV.

### Cell Culture

U2-OS osteosarcoma cells (American Tissue Type Collection HTB96) were grown in Dulbecco's Modified Eagle Medium (DMEM) (Gibco) containing 10% Fetal Bovine

Serum (FBS), 5% Glutamine, 5% Non-Essential Amino Acids (NEAA), 50 µg/mL penicillin, and 50 µg/mL streptomycin (Invitrogen). Cells were maintained under standard conditions at 37 degrees celsius and 5% CO<sub>2</sub> and passaged with Trypsin-EDTA (0.25%) containing phenol red. All cell lines tested negative for mycoplasma and microsatellites authenticated. All cell lines were also confirmed to be free from HPV DNA contamination.

### **Generation of CYLD Knockdown**

U2-OS cells were plated in six-well plates at 70% confluency. Cells were co-transfected with a mix of three CYLD CRISPR/Cas9 knockout (KO) plasmids each encoding the Cas9 nuclease and a target-specific 20 nt guide RNA (gRNA) designed for maximum knockout efficiency and a GFP selection marker as well as a CYLD Homology-Directed Repair (HDR) plasmid that provides a specific DNA repair template for a double strand break, the puromycin resistance gene and an RFP marker. Transfection was performed using Lipofectamine 3000 according to the manufacturer's instructions. 24 hours later, cell viability was confirmed with light microscopy and successful transfection was confirmed by visualizing GFP and RFP expression under fluorescence microscopy. 72 hours following transfection, cells were re-plated at low density into 10 cm dishes and grown in media containing 2 µg/ml puromycin (Invitrogen) for one week. Upon observing isolated colonies of roughly 100 cells, individual clones were collected with trypsinization and transferred to 24-well plates and propagated in media supplemented with 2 µg/ml puromycin. Clones that reached confluency in 24-well plates were subsequently transferred to 6-well plates in duplicate. Cells in one of the wells were used for subsequent analysis and cells in the other were frozen in 10% DMSO in FBS at -80 degrees Celcius.

### **Immunoblotting**

Parental cells and puromycin-selected CYLD Cas9/CRISPR clones were collected by trypsinization and lysed in radioimmunoprecipitation assay (RIPA) lysis buffer (Sigma) with

the addition of protease inhibitors (Roche) and phosphatase inhibitors (Sigma) for 15 minutes on ice. Lysates were then mechanically homogenized with an 18-gauge syringe and insoluble material was removed by centrifugation at 14,000 rpm for 15 minutes at 4 degrees Celsius. Protein concentration was determined using Qubit assay (Invitrogen). 20µg of total protein was mixed with 2X loading Laemmli buffer (Biorad) supplemented with DTT (Sigma) and incubated for 10 minutes at 95 degrees Celsius. Proteins were separated in 4% to 20% Tris-glycine polyacrylamide gels (Mini-PROTEAN; Bio-Rad) and electrophoretically transferred onto polyvinylidene fluoride membranes. Membranes were blocked with 3% BSA in PBS and incubated with primary antibodies against CYLD (Santa Cruz) and phospho-p65 as well as control primary antibodies against GAPDH. Secondary antibodies were conjugated with horseradish peroxidase. After sequential washes in TBST buffer, a chemiluminescent HRP substrate was applied to the membrane and signals were immediately visualized using a ChemiDoc Bio-Rad imager.

### HPV Transfection

CYLD-CRISPR clones, as well as WT U2-OS, cells were grown in duplicates in six-well plates. Clones and CYLD control cells were transfected with either circular HPV DNA or a GFP-containing plasmid, which served as a transfection efficacy control. Transfections were performed using Lipofectamine 3000, according to the manufacturer's protocol. Cell viability and GFP expression were confirmed using light and fluorescence microscopy, respectively, 24 hours after transfection. Samples were incubated for six, nine, and thirteen days and then collected with trypsinization. DNA and RNA were isolated from each of the collected samples. If cells reached confluency, they were split into new plates at medium density.

### Quantitative Real Time PCR

**DNA:** Cells were lysed with Trypsin, pelleted by centrifugation at 1500 x RPM for 5 minutes in growth media, resuspended in PBS and pelleted at 1500 x RPM for 5 minutes.

Low molecular weight DNA was extracted using Modified Hirt Extraction as described in <https://ccrod.cancer.gov/confluence/display/LCOTF/mHirt>. DNA concentration was measured using the Qubit dsDNA HS assay kit and the Qubit 2.0 fluorometer. Quantitative real-time (q-PCR) was performed using the 5ng of DNA and iQ SYBR Green Supermix (Bio-Rad). The following DNA primer pairs were constructed for the E6/E7 and L1/L2 regions of HPV16, as well as the housekeeping gene GAPDH.

**RNA:** Cells were lysed with Trypsin, pelleted by centrifugation at 1500 x RPM for 5 minutes in growth media, resuspended in PBS and pelleted at 1500 x RPM for 5 minutes. RNA was extracted using the RNEasy Spin Miniprep Kit (QIAGEN). 2% 2 M dithiothreitol (DTT) was added to Lysis buffer, and the remaining protocol was followed as specified. Optional DNase I digestion of the lysate was additionally performed. Isolated RNA concentrations were measured using the Qubit RNA BR assay kit and the Qubit 2.0 fluorometer and stored at -80 degrees Celsius. cDNA was synthesized using 1µg of RNA and the iScript cDNA synthesis kit (Bio-Rad). The concentration of cDNA produced was measured as previously specified. Quantitative real-time reverse transcriptase (qRT-PCR) was performed using iQ SYBR Green Supermix (Bio-Rad) and 10ng of cDNA. Primers were constructed against coding regions of E6, E7, and L1 from HPV16, as well as the housekeeping gene GusB. Both DNA and RNA analyses were performed in triplicate. Quantification was performed using the  $\Delta/\Delta C_t$  value method.

### Luciferase Reporter Assay

The luciferase reporter assay was used to measure activity of the NF- $\kappa$ B dependent promoter and the long control region (LCR) of the HPV16 both in CYLD-CRISPR clones and wild-type U2-OS cells. U2-OS CYLD-CRISPR clones as well as U2-OS control cells



were plated in triplicate in flat-bottom 96-well cell culture plates. Cells were transfected with either the 3kb-con-luc plasmid or p5193 pGL4-LCR-HPV16-LCR (nt 7000-100)-luc plasmid (Addgene pl. 32888) to measure NF- $\kappa$ B and LCR activity in CYLD depleted and wild-type U2-OS cells, respectively. Luciferase expressing plasmid lacking promoter binding sites (3kb-luc) was used as a normalization control in both experiments. Lipofectamine 3000 was used for all transfections, according to the manufacturer's protocol. In the NF- $\kappa$ B experiment, cells were grown in either DMEM or DMEM supplemented with 1 ng/uL (0.1%) TNF- $\alpha$  to induce NF- $\kappa$ B activity. To measure luciferase production, cells were rinsed with PBS and lysed in 1X Cell Culture Lysis Reagent (Promega). In the NF- $\kappa$ B experiment, protein concentration was measured for each well using the Qubit Protein assay kit and the Qubit 2.0 fluorometer in order to normalize results. 100uL of luciferase assay buffer mixed with luciferase assay substrate (Promega) was added to each well and luciferase production was immediately measured using a microplate reader Tecan.

## *Results*

### **TRAF3 and CYLD are mutated in a subset of HPV-positive HNSCC**

The Cancer Genome Atlas (TCGA) has contributed to our understanding the molecular basis of cancer through comprehensive genetic analysis (whole genome sequencing, RNA sequencing, methylation profiles) of many human cancers, including HNSCC. For HNSCC, TCGA sequenced both HPV-positive and HPV-negative tumors. We previously reported that almost 36% of HPV-positive tumors in the initially analyzed cohort (n=36) had mutations in TRAF3 or CYLD. TRAF3 is an adapter that complexes proteins on the intracellular surface of receptors involved in inflammation and immune response signaling. It also has an E3 ubiquitin ligase activity. CYLD is a deubiquitinating enzyme that also has activity in immune signaling. Interestingly, TRAF3 and CYLD are both negative regulators of the transcription factor NF- $\kappa$ B, which is the major orchestrator of the immune response. Thus, while TRAF3 and CYLD have opposite actions with respect to ubiquitin, these actions both serve to dampen the activation of an immune response.<sup>40,48,49</sup>

Our analysis of the expanded HNSCC TCGA identified that 28% of HPV-positive head and neck tumors (n=65) harbored defects in TRAF3 or CYLD. The majority of TRAF3 alterations (78%) were homozygous deletions, while the remainder (22%) were truncating mutations (Figure 4A). Likewise, most of CYLD genetic variations (78%) were deletions or truncating mutations, with the rest comprising missense mutations affecting its ubiquitin hydrolase catalytic domain or lying in close proximity to a critical protein binding

site (Figure 5B). The copy number status of mutated CYLD or TRAF3 revealed a shallow loss (heterozygous deletion) in all samples with point mutations, further supporting loss of function in these tumors.

In contrast, both genes were mutated in about 2% of HPV-negative HNSCC (Figure 4B). Notably, some of these mutations are amplifications which would have the opposite effect to the exclusively inactivating mutations seen in the HPV-positive cohort. Interestingly, TRAF3 was mutated in 4% of uterine cervical cancers studied by TCGA, of which 37.5% were amplifications, while CYLD was mutated in only 2% (Figure 4C). Pan TCGA analyses revealed inactivating mutations in TRAF3 or CYLD were infrequent in solid cancers, occurring in 10% or more of tumors only in diffuse large B-cell lymphoma. These data suggest that TRAF3/CYLD play an exclusive role in HPV-positive head and neck cancer among the solid tumors studied.

### **TRAF3/CYLD inactivation is associated with improved survival in HPV-positive HNSCC**

Compared to patients with tobacco-associated HPV-negative HNSCC, those with HPV-positive HNSCC have better overall survival and improved response to treatment, which usually consists of chemo- and radiation therapy; however, survivors frequently suffer from life-long treatment-associated toxic side effects, such as swallowing and speech dysfunction. Moreover, approximately 25% of HPV-positive HNSCC patients develop recurrent or metastatic disease, for which there are currently no curative treatment options available. An increasing clinical interest is to decrease the morbidity of therapy for HPV+ HNSCC through treatment de-escalation, however, the current lack of biomarkers that could help identification of HPV-positive patients with good prognosis prevents appropriate patient assignment for deintensified therapy. To determine a significance of TRAF3/CYLD mutations in HPV-positive HNSCC, we performed Kaplan-Meier survival analysis in TCGA cohort of HNSCC patients based on TRAF3/CYLD mutations and HPV status. Remarkably, TRAF3 or CYLD mutations strongly correlated with improved overall survival vs.

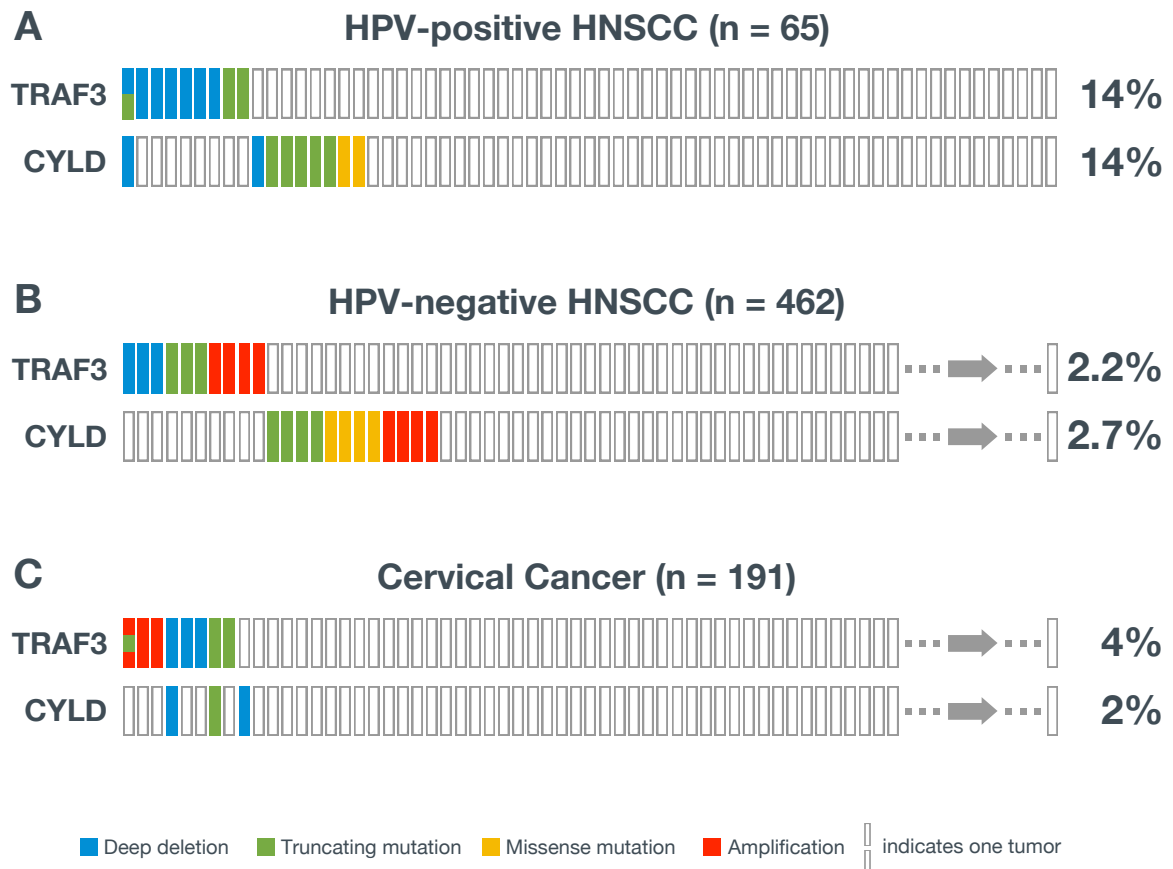


**Figure 4.** TRAF3/CYLD genetic alterations in HPV-positive HNSCC, HPV-negative HNSCC, and cervical cancer. TCGA contains detailed sequencing information on HPV-positive HNSCC (n=65), HPV-negative HNSCC (n=462), and cervical cancer (n=191); the rates of TRAF/CYLD genetic alterations (deep deletion (blue), truncating mutation (green), missense mutation (yellow), and amplification (red)) in these three tumor types were assessed using cBioPortal. (A) HPV-positive HNSCC showed an increase rate of TRAF3/CYLD mutations, with 14% of tumors exhibiting mutations in each gene. Except for one tumor, these mutations were mutually exclusive. In addition, all truncating and missense point mutations were inactivating. (B) On the other hand, in HPV-negative HNSCC, 2.2% of tumors contained TRAF3 mutations while 2.7% of tumors contained a CYLD mutation. There was a mix of amplifications and inactivating mutations for both genes. Among 191 cervical tumors assessed, 4% had TRAF3 mutations, including amplifications, and 2% of tumors had CYLD mutations (C). Graphs were adapted from cBioPortal.

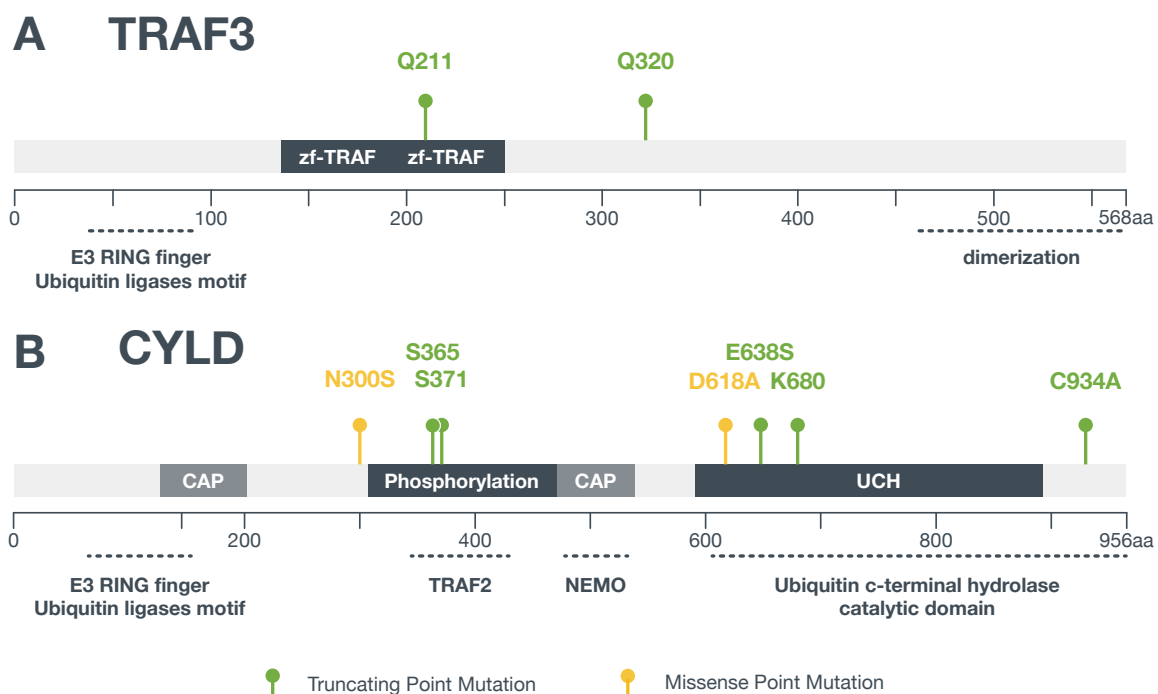


**Figure 5. Schematic of TRAF3/CYLD Mutations in HPV-HNSCC.** (A) Two truncating mutations in TRAF3 were identified in HPV-HNSCC. (B) Five truncating mutations and two missense point mutations were observed in CYLD. These mutations. zf indicates a zinc finger domain. CAP indicates a cytoskeletal-associated protein domain. “Phosphorylation” indicates a phosphorylation site, and UCH indicates a ubiquitin C-terminal hydrolase. (See Figure 4, adapted from cBioPortal)

HPV-positive tumors lacking TRAF<sub>3</sub>/CYLD mutations ( $p=0.03$ ) and when compared to patients with HPV-negative tumors ( $p=0.008$ ) Survival of patients with HPV-positive tumors that were wild type for TRAF<sub>3</sub> and CYLD was similar to survival of patients with HPV-negative HNSCC ( $p=0.27$ ) (Figure 6).

### **TRAF<sub>3</sub>/CYLD were preferentially mutated in an independent HPV-positive HNSCC cohort**

In order to validate the results of TCGA, HNSCC patients who were operated on at Yale-New Haven Hospital were assessed for the HPV-status. A cohort of 21 HPV-positive HNSCC tumors and three HPV-negative tumors were ultimately studied. Genomic sequencing of tumors revealed that five of the 21 tumors (22%) had mutations in either TRAF<sub>3</sub> or CYLD. The remaining 18 tumors (78%) had WT TRAF<sub>3</sub>/CYLD. TRAF<sub>3</sub>/CYLD mutations tended to be associated with male gender (80% vs. 72%), smoking status (40% vs. 33%), advanced clinical stage (100% vs. 55.5% Stage IV or higher) and were inversely associated with recurrence (20% vs. 28%). However, because the sample size of this cohort was limited, none of these comparisons were statistically significant (Table 1). Finally, because all patients studied in this cohort were currently alive, it was not possible to make any determination about the association between TRAF<sub>3</sub>/CYLD mutations and long-term survival.

Genomic sequencing of these tumors showed that nine of 21 (43%) had alterations in NF- $\kappa$ B pathway genes. Specifically, five of 21 (22%) of tumors had alterations in TRAF<sub>3</sub>/CYLD. In two of these five tumors, TRAF<sub>3</sub>/CYLD mutations were overlapping. Mutations in TRAF<sub>3</sub>/CYLD were either deep deletions (5), truncations (1), or missense mutations (1). In addition, one tumor (4.8%) had a frameshift mutation in TRAF<sub>2</sub> while another tumor (4.8%) had a truncating mutation in cIAP<sub>2</sub>. Two tumors (9.5%) had missense mutations in NIK. No mutations were seen in MYD88, NFKB1A, TNFAIP<sub>3</sub>, TRAF<sub>6</sub>, and cIAP<sub>1</sub>. Also, no amplifications were seen in this cohort. In addition, alter-

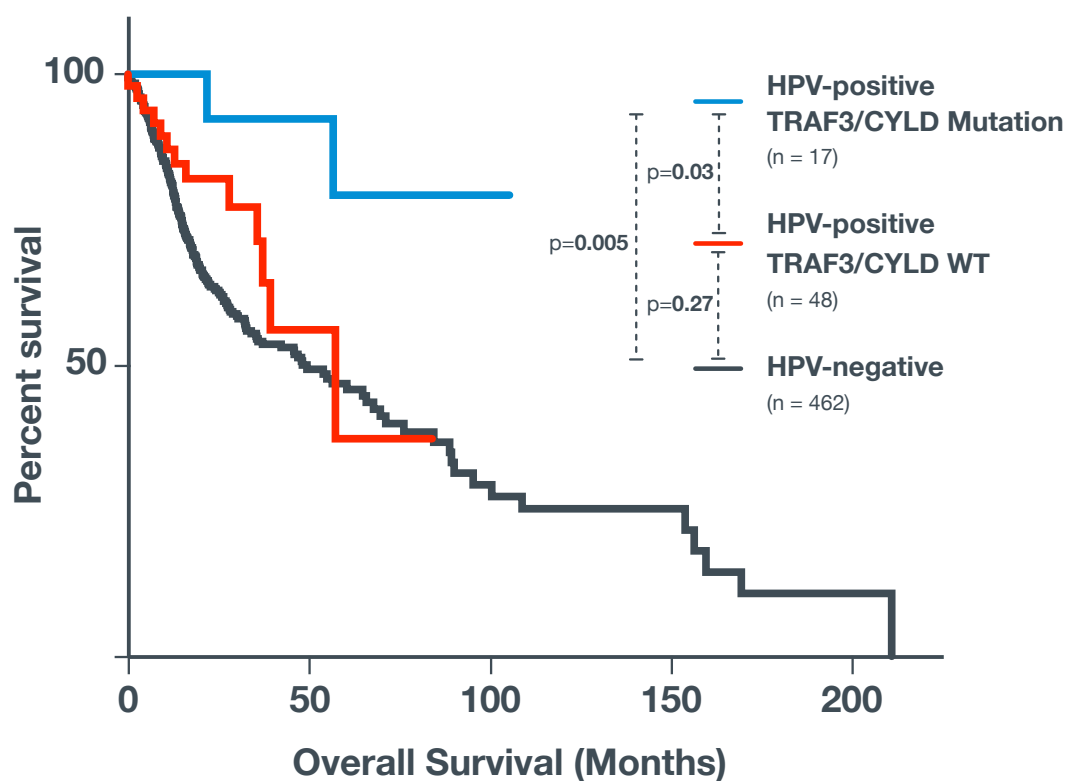


**Figure 6.** Kaplan–Meier Survival Curves of HNSCC Patients in TCGA Cohort. Survival data was obtained for 527 HNSCC patients in TCGA cohort. Among these, 462 patients had HPV-negative HNSCC (Black) and 65 patients HPV-positive HNSCC. HPV-positive patients were further stratified on the TRAF3/CYLD mutation status (mutant: Blue, n=17; wild-type: Red, n=48). Patients with TRAF3/CYLD mutant HPV-positive HNSCC showed improved survival as compared to HPV-positive HNSCC patients with WT TRAF3/CYLD tumors ( $p=0.03$ ) or HPV-negative HNSCC patients ( $p=0.005$ ). There was no statistically significant difference between HPV-positive patients with WT TRAF3/CYLD and HPV-negative patients ( $p=0.27$ ).

	TRAF3/CYLD WT	TRAF3/CYLD Mutated
	n=18 (78%)	n=5 (22%)
Median Age	60.5	58
Male	13 (72%)	4 (80%)
Female	5 (28%)	1 (20%)
Smokers	6 (33%)	2 (40%)
Stage II	2 (11%)	
Stage III	2 (11%)	
Stage IV	1 (5.5%)	
Stage IVA	9 (50%)	4 (80%)
Stage IVB	1 (5.5%)	1 (20%)
Recurrence	5 (28%)	1 (20%)

**Table 1. Demographic and Clinical Characteristics of Yale Cohort.** Tumors of 21 HPV-positive HNSCC patients who underwent surgery at Yale-New Haven Hospital were analyzed for NF- $\kappa$ B pathway mutations. In addition, patient records were queried for demographic information including age at diagnosis, smoking status, clinical stage, and recurrence. Mutations were observed in 5 (22%) of tumors. Due to low sample size, statistical significance could not be obtained for each comparison.

ations seen in TRAF3/CYLD were mutually exclusive to those in the other genes. (Figure 7.

### CYLD was depleted in a U2-OS in vitro model

To begin determine a role of CYLD in the HPV-associated carcinogenesis, we developed CYLD knockdown cells using Cas9/CRISPR system (Santa Cruz, see Methods). We chose U2OS cells for these experiments, because they have wild type TP53 and RB genes (characteristics of HPV-positive cancer cells) and because they support HPV replication and have the same HPV gene expression profile after HPV introduction as keratinocytes



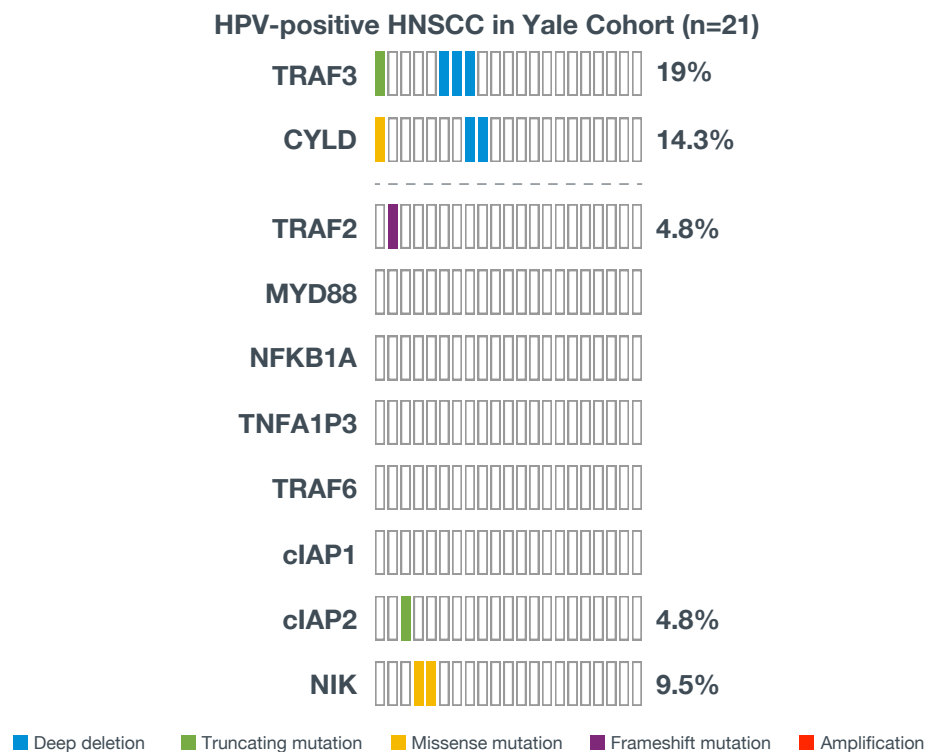


**Figure 7.** NF- $\kappa$ B Pathway Mutations in HPV-positive HNSCC in the Yale Cohort. 21 HPV-positive HNSCC tumors isolated from patients who underwent surgery at Yale-New Haven Hospital were sequenced for the presence of NF- $\kappa$ B pathway mutations. As in TCGA, TRAF3 and CYLD were the most frequently mutated with two tumors exhibiting concurrent mutations in both genes. Two tumors (9.5%) had missense mutations in NIK. One tumor (4.8%) had a frameshift mutation in TRAF2 while another tumor (4.8%) had a truncation in cIAP2.

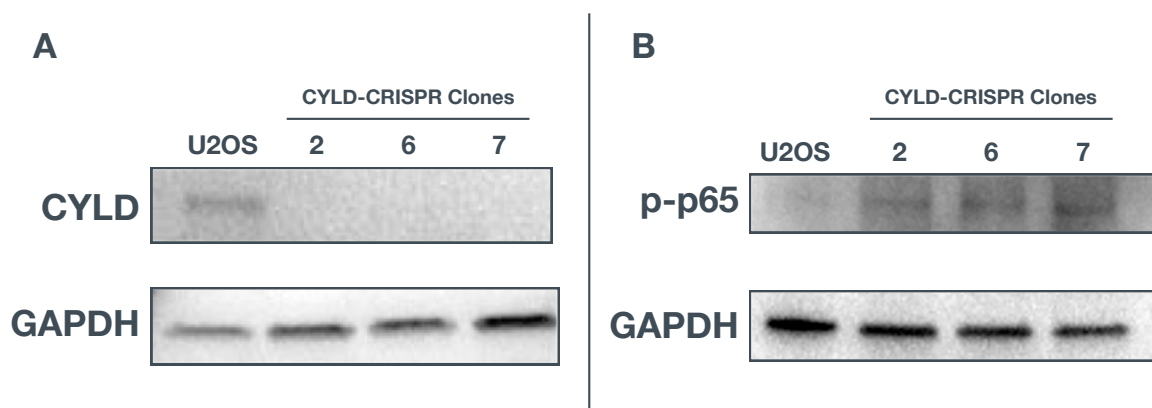


**Figure 8.** Immunoblotting of CYLD and phosphorylated p-65 in WT and CYLD deleted U2-OS cells. Immunoblotting of CYLD and phosphorylated p-65 in WT and CYLD deleted U2-OS cells. Immunoblotting was performed to confirm knockdown of CYLD after CRISPR/Cas9 mediated deletion. Total cellular lysates from stable CYLD-CRISPR clones (2, 6, and 7) or WT U2-OS cells were immunoblotted with antibodies against CYLD (A) and phosphorylated p-65 (B); GAPDH was used as a loading control (see Methods).

that are natural targets of HPV infection.<sup>52,53,54,55</sup> Confirmation of CYLD knockdown was established in a multi-step process. First, GFP and RFP expression were observed in transfected cells 72 hours after introduction of the plasmids, confirming effective delivery of both KO and HDR constructs. Next, viable cell clones were collected and expanded under puromycin selection, and finally, immunoblotting with antibodies against CYLD was performed and revealed complete loss of CYLD expression in three chosen clones (Figure 8A).

### CYLD-depletion leads to NF- $\kappa$ B over-activation in vitro

NF- $\kappa$ B activation is a hallmark feature of many tumors, as this factor is involved in enhanced cell proliferation, angiogenesis, and metastasis and the inhibition of differentiation and apoptosis. In order to ensure the robustness of our model, we first confirmed that the expected NF- $\kappa$ B pathway activation was recapitulated in vitro. First, immunoblotting was performed to detect the phosphorylated NF- $\kappa$ B subunit p65, a marker for activated NF- $\kappa$ B. GAPDH was used as a control. Compared to control cells, p-p65 was increased in all three of the CYLD-CRISPR clones studied. These data strongly suggest that of NF- $\kappa$ B

was activated following CYLD depletion (Figure 8B).

To confirm activation of NF- $\kappa$ B in CYLD Cas9/CRISPR clones, a luciferase reporter plasmid containing three copies of a NF $\kappa$ B-binding promoter element upstream of luciferase was used. As a control, we transfected luciferase containing plasmids without the NF- $\kappa$ B binding element in the promoter and also normalized all samples for protein concentration. NF- $\kappa$ B activity was increased six-fold, three-fold, and six-fold in clones 2, 6, and 7, respectively. Upon treatment with a potent NF- $\kappa$ B activator TNF- $\alpha$ , NF- $\kappa$ B activity was increased 102-fold, 90-fold, and 281-fold over the untreated baseline and two-fold, two-fold, and seven-fold over the TNF- $\alpha$  baseline in clones 2, 6, and 7, respectively. The fold difference in NF- $\kappa$ B activity reached statistical significance in clones 2 and 7 in the untreated experiment and in all three clones in the treated experiment. Overall, these data suggest that CYLD depletion increased both exogenous and inducible NF- $\kappa$ B activity (Figure 9). While active NF- $\kappa$ B is a known consequence of CYLD depletion, these data support faithful recapitulation of this pathway in our in vitro model.

### HPV DNA is maintained at a higher level in CYLD-CRISPR cells

The goal of constructing an in vitro model of CYLD depletion is to better characterize how loss of CYLD activity may affect HPV infection and the establishment of head and neck cancer. To do so, we first aimed to study HPV replication in the CYLD-CRISPR model. We first synthesized circular HPV DNA. We then designed an experiment in which this HPV DNA was introduced into CYLD-CRISPR clones as well as into control U2-OS cells. Clones 2 and 7 were chosen for this analysis as they had the highest levels of NF- $\kappa$ B activity (Figure 9).

Cell cultures in duplicates were transfected with a circular HPV, or GFP-containing plasmid as a control, to ensure reliable and consistent transfection efficacy between clones. Cells were cultured for six, nine, and thirteen days after transfection, after which HPV DNA was isolated and measured using qPCR.

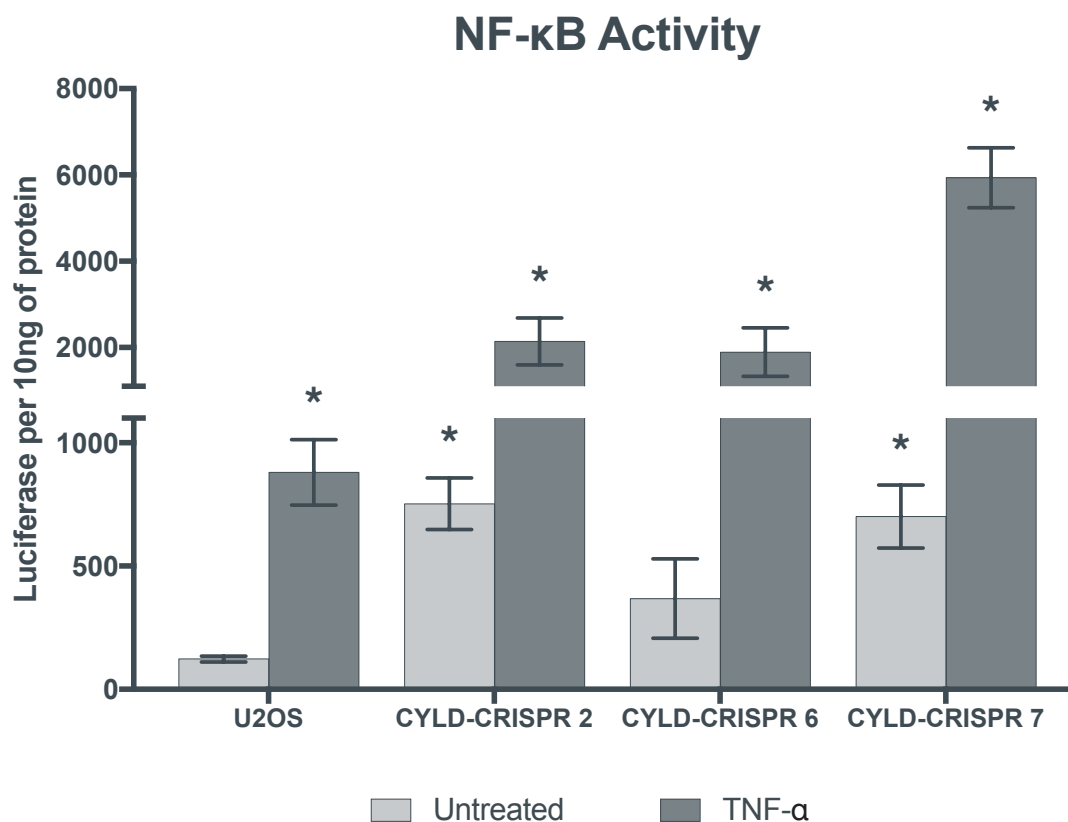


**Figure 9.** NF- $\kappa$ B activity in CYLD-CRISPR clones and WT U2-OS cells. NF- $\kappa$ B activity was measured in WT U2-OS cells and CYLD-CRISPR clones 2, 6, and 7 treated or not treated with TNF- $\alpha$  (1 ng/uL) using a luciferase reporter assay (see Methods). (\*) indicate statistical significance of  $p < 0.05$ .

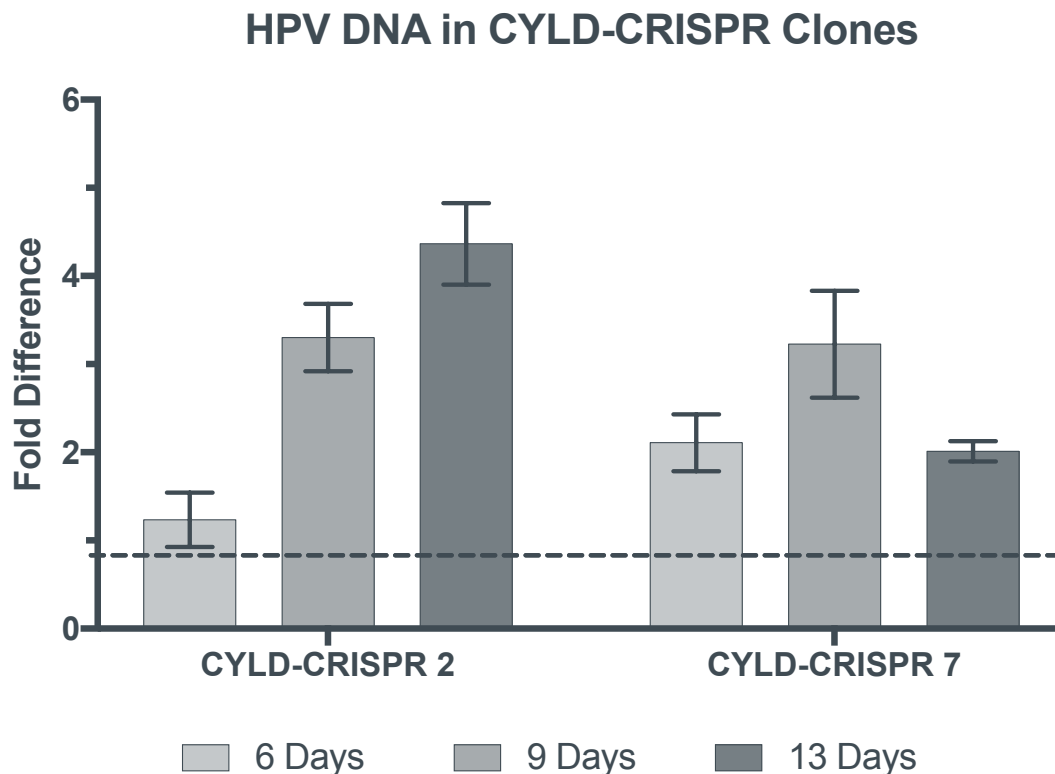


**Figure 10.** HPV DNA at various time points in CYLD-CRISPR clones. WT U2-OS as well as CYLD-CRISPR clones 2 and 7 were transfected with circular HPV DNA and the amount of HPV DNA was measured 6, 9, and 13 days following transfection (see Methods). HPV DNA is shown relative to the amount seen in U2-OS parental cells (dotted line at fold difference = 1).

GFP transfection revealed similar 60% transfection efficiency in all cell cultures tested. At 6 days, clones 2 and 7 had 1.2-fold and 2.1-fold increases in HPV DNA when compared to U2-OS control cells, respectively. At 9 days, this increase was 3.3-fold and 3.2-fold, respectively. At 13 days, the increase was 4.3-fold and 2.0-fold, respectively. While further work is required to elucidate the variability in fold-increase in the two clones at various time points, there was a consistent increase in the relative amount of HPV DNA in CYLD depleted cells compared to U2-OS control cells. These data suggest that HPV DNA is maintained at a higher level in a CYLD depleted cells. Furthermore, these data support the notion that NF- $\kappa$ B activity is directly or indirectly involved in the maintenance of HPV episomes (Figure 10).

### HPV LCR activity appears to be increased in a CYLD depleted model

We hypothesized that CYLD depletion and NF- $\kappa$ B activation contribute to HPV replication and that this phenomenon may help explain the association between these mutations and head and neck carcinogenesis. To further elucidate the first part of this hypothesis, we performed an experiment in which a luciferase reporter assay specific to the HPV long control region (LCR) was tested in CYLD-CRISPR clones as well as control U2-OS cells. The long control region contains the HPV early promoter that regulates transcription of the oncogenes E6 and E7 among other HPV promoters and HPV regulatory elements (Figure 2).

LCR activity was increased 11-fold and 24-fold over U2-OS control cells 24 hours, in clones 2 and 7 respectively. At 48 hours, this increase was nine-fold and 17-fold respectively. At 72 hours, the increase was four-fold and 11-fold, respectively. Finally, at 96 hours, the increase was nine-fold and 18-fold, respectively. All fold-increases in LCR activity in the CRISPR clones over U2-OS control cells achieved statistical significance. These data suggest that CYLD deletion results in a significant increase in HPV LCR activity in our in vitro model. Additional experiments should be performed to elucidate the variability in fold-increases; however, a clear relationship between CYLD-deletion and transcriptional activity of the LCR has been established (Figure 11).

In summary, we developed an in vitro model of CYLD inactivation in the U2-OS cell line and demonstrated that NF- $\kappa$ B was transcriptionally active in this model. Upon introduction of episomal HPV to CYLD-deleted cells, we showed an increase in the amount HPV DNA that was sustained for a period of up to 13 days. Finally, we found that transcriptional activity driven by the HPV LCR is increased in CYLD-deleted cells as compared to parental cell line. Together, these data support a model of increased HPV replication and episomal maintenance that is predicated on NF- $\kappa$ B activation in the setting of removal of negative regulators.

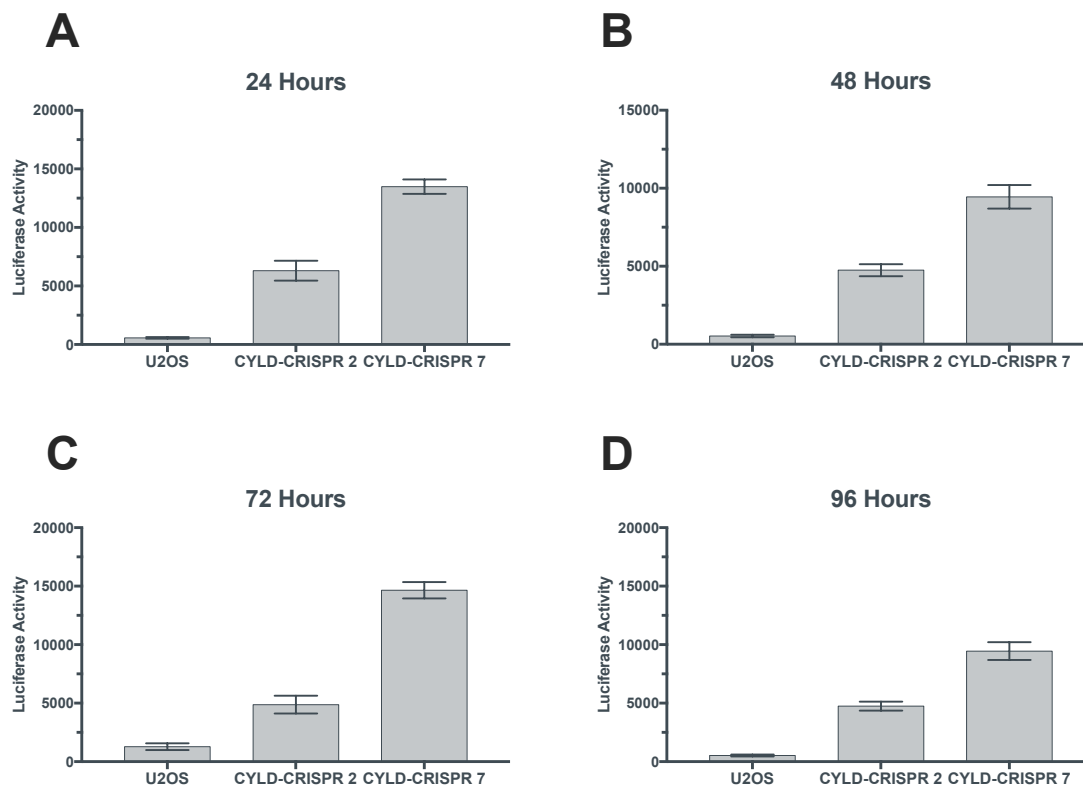


**Figure 11.** LCR Activity in CYLD-CRISPR Clones compared to WT U2-OS Cells. Transcriptional activity of the HPV16 long control region (LCR) was measured in WT U2-OS cells and CYLD-CRISPR clones 2 and 7 using a luciferase reporter assay (see Methods). Activity was measured at 24, 48, 72, and 96 hours following transfection with the luciferase plasmid. At all four time points, CYLD-CRISPR clones 2 and 7 showed increased LCR activity.

## *Discussion*

THE OVERALL AIM OF OUR WORK is to understand how HPV causes head and neck cancer. It is currently known that head and neck cancer can arise from persistent and untreated HPV infections or independent of HPV entirely—usually as a result of tobacco and alcohol exposure.<sup>2</sup> Moreover, it is known that the mechanisms that cause HPV-positive and HPV-negative HNSCC are distinct, as are the clinical features of both types of tumors. In addition to understanding tumor biology, it is also imperative to develop a better understanding of which treatments are beneficial for which patients. Against a backdrop of rising incidence, it is important to re-examine whether current treatment guidelines are appropriate.

While it is known that HPV-positive cancers of the head and neck portend favorable prognosis relative to their HPV-negative counterparts at a population level, there is currently no way to determine whether a specific HPV-positive HNSCC requires the intensive chemoradiation regimen that is the current standard of care.<sup>11</sup> To an individual patient, this epidemiological statistic provides little comfort, given that a notable minority of these tumors continue to have aggressive behavior that evades best available therapies. However, for a majority of them, it is likely that the high doses of chemoradiation are more than would be required to achieve a curative response.<sup>56,57,58,59</sup>

In addition, given that HPV-positive head and neck cancer patients tend to be younger and healthier, they have additional time to develop long-term sequelae of treatment.<sup>58</sup> De-



veloping a reliable biomarker that can identify which patients have a more treatment- responsive variant of HPV-positive HNSCC is currently a major aim of head and neck oncology.<sup>56</sup> Developing such a biomarker could potentially inform clinical trials that allow some HPV-positive HNSCC patients to undergo lower doses of chemoradiation, achieving oncologic cure without the excessive morbidity of treatment.

Finding this biomarker requires both observing factors that are associated with improved survival in HPV-positive HNSCC and also understanding how cancer biology differs as a result of those factors. Our laboratory previously identified genes that were preferentially mutated in HPV-positive HNSCC and that these genes had a common downstream effect—activation of NF- $\kappa$ B.<sup>40,48,49</sup> While several mutations were discovered, TRAF3 and CYLD were by far the most prevalent. Interestingly, these mutations correlated with improved survival, the lack of HPV integration, and a unique genomic and proteomic profile.<sup>12</sup>

The E6/E7 driven inactivation of p53 and Rb represents the classical mechanism for HPV-driven carcinogenesis and is by far the most studied pathway of cancer development due to HPV. In this classical pathway, genomic integration of HPV is thought to be the principal event that allows E6/E7 expression and subsequent oncogenesis to ensue.<sup>21,60</sup> The discovery of a subset of HPV-positive tumors containing mutations associated with a lack of integration suggests that a different pathway of malignant transformation may be in play.<sup>12,18</sup> In fact, it is possible that p53/Rb suppression and NF- $\kappa$ B activation represent a distinct and potentially mutually exclusive pathways to cancer. NF- $\kappa$ B activation is a hallmark feature in many cancers. Furthermore, chronic inflammation, which leads to organic increases in NF- $\kappa$ B has been linked to cancer in several organs. However, the development of cancer as a result of NF- $\kappa$ B pathway mutations is rare, especially in solid tumors.<sup>61,62</sup> Thus, our findings led us to hypothesize that a subset of HPV-positive HNSCC arise from a novel mechanism of carcinogenesis.<sup>18,5</sup> We further posited that mutations in TRAF3 or CYLD could serve as biomarkers to identify patients who could be candidates for therapeutic de-escalation.

To further study our proposed non-canonical pathway of HPV-driven carcinogenesis, we decided to develop an *in vitro* model based on CYLD inactivation. TRAF3 and CYLD were suitable candidates given that the majority of NF- $\kappa$ B activating mutations were observed in these two genes, and CYLD was chosen for initial analysis. We chose to delete CYLD in the U2-OS cell line. From a technical perspective, U2-OS cells support HPV replication *in vitro*. In fact, U2-OS is a well-established cell line for the study of HPV infection. Furthermore, following the introduction of HPV genomes, expression of HPV genes is similar in U2-OS cells and keratinocytes naturally infected by the virus.<sup>52,53,54,55</sup>

In this study, we demonstrated the following: First, we deleted CYLD in U2-OS cells using the CRISPR/Cas9 system. We developed three stable clones with CYLD knockdown confirmed by Western Blot (Figure 8A). Second, we demonstrated that phosphorylated-p65 was increased in each CYLD-CRISPR clone, indicating activation of NF- $\kappa$ B (Figure 8B). Third, we followed up our previous result by demonstrating functional activation of NF- $\kappa$ B by observing increased endogenous and TNF  $\alpha$ -induced NF- $\kappa$ B activity in a luciferase reporter assay (Figure 9). Fourth, we showed that HPV DNA is maintained at a higher level in CYLD-CRISPR cells across various clones and time points (Figure 10). These results were consistent with increased HPV DNA replication in the absence of CYLD. Finally, we showed that activation of the HPV long control region (LCR) was dramatically increased after CYLD depletion through a luciferase reporter assay (Figure 11). Thus, our data support our proposed model in which CYLD inactivation results in activation of NF- $\kappa$ B, increased replication, and maintenance of episomal HPV.

### Limitations of Current Study

Our study has several limitations to be addressed in future experiments. First, a natural limitation of using a tumorigenic cell line such as U2-OS is its inability to faithfully recapitu-

late de novo carcinogenesis. However, the fact that U2-OS cells harbor wild-type versions of the major tumor suppressors p53 and Rb means that U2-OS can be used as a pilot cell line for initial experimentation.<sup>52,53,54,55</sup>

Second, in our experiment measuring HPV DNA in CYLD-CRISPR cells after introduction of circular HPV genomes, we were unable to restrict bacterial DNA. Because we wanted to measure the amount of new HPV DNA synthesized in vitro, bacterial DNA could alter our qPCR results. We attempted digesting DNA samples with DpnI to remove methylated DNA but were unable to obtain usable DNA concentrations subsequently. We addressed this issue by taking DNA at time points after 6 days. As Lipofectamine 3000 transfection is transient, we hypothesized that HPV DNA that is measured at minimum 144 hours after transfection is unlikely to have bacterial DNA at a significant level.

Third, in our experiment testing LCR activity in CYLD-CRISPR cells using a luciferase reporter assay, we were unable to measure protein concentrations of the samples measured. Protein concentrations are used as a normalization control to account for any differences in light production of a particular sample having more cells. While this makes our presented data preliminary, we still believe it is reliable because each well was plated at the same density, confirmed to be viable after plating and transfection, and lysed under the same conditions. Therefore, it is unlikely that a large difference in cell counts between samples would confound the results in a meaningful manner.

Fourth, our method of introducing HPV DNA into cells was through transfection of circular HPV genome using Lipofectamine 3000. Though we optimized this protocol to ensure good transfection efficacy and cell survival following transfection, this process deviates from natural HPV infection in several ways. However, recapitulating natural HPV infection is notoriously difficult in vitro because establishment of infection requires keratinocytes undergoing active differentiation. This could be accomplished using organotypic raft cultures made from epithelial cells and pseudoviruses, which will be discussed later.

## Future Directions

A number of future studies can be performed to confirm and expand upon our preliminary findings. This future work can be broadly divided into five areas. First, while analysis of the complete TCGA cohort led to the initial discovery that TRAF3 and CYLD were preferentially mutated in HPV-positive HNSCC, this finding needs to be validated in an independent cohort. Second, we need to repeat our preliminary analyses in a TRAF3 model in order to confirm our expectation that TRAF3/CYLD depletion leads to similar downstream outcomes. A number of other NF- $\kappa$ B pathway mutations, while observed with less frequency clinically, should also be tested as a part of this aim. Third, additional experiments will need to be conducted using in vitro models of TRAF3 and CYLD depletion to further characterize the relationship between increased NF- $\kappa$ B activity and the maintenance, replication, and integration of HPV. Fourth, the future aim of this work is to determine whether TRAF3/CYLD depletion and resultant NF- $\kappa$ B activation can actually lead to tumorigenesis in in vitro and in vivo models. And finally, if these experiments yield positive results, then prospective randomized trials should be designed to evaluate the efficacy of TRAF3/CYLD as biomarkers in selecting HPV-positive HNSCC patients for therapeutic de-escalation.

The Cancer Genome Atlas provided valuable information about 65 HPV-positive and 462 HPV-negative HNSCC and led to the finding that between one quarter and one third of HPV-positive tumors have mutations in NF- $\kappa$ B regulators such as TRAF3 and CYLD. The Eastern Cooperative Oncology Group Trial (ECOG) 1308 trial (E1308) recently studied 80 HPV-positive tumors in a therapeutic de-escalation trial comparing reduced radiation doses to standard of care.<sup>63</sup> Patients who responded to induction chemotherapy were offered lower doses of radiation while patients who did not achieve a complete clinical response were given standard radiation dosages. 53 patients received lower dose radiation. Our laboratory has been able to obtain access to samples from these 80 tumors with the plan of conducting genomic analyses to determine the mutation status of TRAF3 and

CYLD.

The addition of these 80 tumors to our analysis will allow us to describe the largest analysis of TRAF3/CYLD alterations in head and neck cancer to date, and provide additional support to our proposed alternative model of HPV-driven carcinogenesis by verification of our initial findings in an independent cohort.

The *in vitro* work that has been previously described was related to CYLD. We previously demonstrated that HPV DNA was maintained at a higher level following CYLD depletion. However, our preliminary data was limited in its ability to determine whether there was active replication of the HPV genome. We could perform Southern Blotting to determine whether HPV replication was increased in the CYLD-CRISPR model. Furthermore, we plan to measure expression of HPV genes such as E1, E2, E6, E7, L1, L2, as well as splice variants associated with viral replication using qRT-PCR.

In addition, our laboratory has constructed a similar model for TRAF3 depletion in the U2-OS cell line using CRISPR/Cas9. While we previously used qRT-PCR and immunoblotting to confirm CYLD-depletion, an additional layer of confirmation could be performed by introducing TRAF3 and CYLD expressing plasmids to their respective deleted clones. We would then perform immunoblotting to ensure restored expression of TRAF3 and CYLD respectively and reduced phosphorylation of NF- $\kappa$ B subunit p65. Furthermore, we would look for a restoration of initial NF- $\kappa$ B activity after re-expression of TRAF3 or CYLD in Cas/CRISPR clones in a luciferase reporter assay. This would further support our conclusion that CYLD depletion is directly responsible for NF- $\kappa$ B activation.

After repeating the previously described experiments in the TRAF3-CRISPR model, we plan to develop novel *in vitro* models in a non-cancerous cell line that can be used to more faithfully recapitulate *de novo* carcinogenesis. For this purpose, we will use human oral keratinocytes (HOK) immortalized by hTERT expression. In addition to TRAF3/CYLD, this protocol can be applied to the number of other NF- $\kappa$ B regulators if

they found inactivated in HPV-associated HNSCC. The advantage of using a keratinocyte cell line is that these cells are the actual targets of HPV infection and also non-cancerous, creating a more accurate model to study carcinogenesis.<sup>52,53,54,55</sup> These cells can also be cultured into organotypic rafts, which allow for three-dimensional growth of cell cultures that more closely resemble in vivo tissues.<sup>64,65</sup>

In order to ensure that our results are not on account of method of HPV delivery, we plan to use HPV Pseudovirus (PsV). Our lab has experience in the construction of HPV PsV using 293TT cells and density gradient centrifugation. Furthermore, the aforementioned raft cultures can support viral replication following infection with HPV PsV.

After confirming that deletion of TRAF3 and CYLD in HOK cells has similar effects on NF- $\kappa$ B activity and transcriptional activity of the LCR, the next phase of our work is to establish whether these genetic alterations predispose cells to develop into tumors. While there is an established link between NF- $\kappa$ B activation and carcinogenesis in tumors such as multiple myeloma, the mechanistic link between these two phenomena remains unclear in HPV-positive HNSCC. Notably, there are a number of features that distinguish normal cells from cancer cells. Cancer cells proliferate without control, do not exhibit anchorage-dependent growth, and suppress apoptosis. HOK, HOK TRAF3- CRISPR, and HOK CYLD-CRISPR with and without introduction of HPV16 will be tested for these features. Cell proliferation, clonogenic survival, and anchorage independent growth will subsequently be studied using available in vitro assays.

A final aim of our work will be to inform prospective clinical trials. While ECOG 1308 tested therapeutic de-escalation, patients were stratified on the basis of response to three cycles of induction chemotherapy. Thus, there are currently no indications for selecting patients for lower radiation doses prior to the initiation of treatment. Here, we propose a prospective trial in which patients with HPV-positive HNSCC and NF- $\kappa$ B pathway mutations are randomized into low-dose and standard-dose radiation groups. The outcomes studied can be progression free survival, as in ECOG 1308, as well as long-term seque-

lae of radiation such as speech and swallowing dysfunction. Powering such a trial will be challenging given that 30% of HPV-positive HNSCC patients have mutations in these genes. However, establishment of therapy guiding biomarkers in HPV-positive HNSCC can change the treatment paradigm in this disease. As incidence rises, personalized and targeted therapy specific to each patient and tumor profile can go a long way towards reducing mortality and morbidity. Furthermore, the aims of our future work present the opportunity to contribute to scientific innovation and better our understanding of human cancer biology.

## References

- [1] Goon, P. K. *et al.* HPV head and neck cancer: a descriptive update. *Head Neck Oncology* 1, 36.
- [2] Marur, S. & Forastiere, A. A. Head and Neck Cancer: Changing Epidemiology, Diagnosis, and Treatment. *Mayo Clinic Proceedings* 83, 489–501.
- [3] Epstein, J. B. *et al.* Quality of life and oral function following radiotherapy for head and neck cancer. *Head Neck* 21, 1–11.
- [4] Syrjänen, K., Syrjänen, S., Lamberg, M., Pyrhönen, S. & Nuutinen, J. Morphological and immunohistochemical evidence suggesting human papillomavirus (HPV) involvement in oral squamous cell carcinogenesis. *International Journal of Oral Surgery* 12, 418–424.
- [5] Network, T. C. G. A. Comprehensive genomic characterization of head and neck squamous cell carcinomas. *Nature* 517, 576.
- [6] Kobayashi, K. *et al.* A Review of HPV-Related Head and Neck Cancer. *Journal of Clinical Medicine* 7, 241.
- [7] Chaturvedi, A. K. & Zumsteg, Z. S. A snapshot of the evolving epidemiology of oropharynx cancers. *Cancer* 124, 2893–2896.
- [8] Gooi, Z., Chan, J. Y. K. & Fakhry, C. The epidemiology of the human papillomavirus related to oropharyngeal head and neck cancer. *The Laryngoscope* 126, 894–900.
- [9] Boscolo-Rizzo, P. *et al.* The evolution of the epidemiological landscape of head and neck cancer in Italy: Is there evidence for an increase in the incidence of potentially HPV-related carcinomas? *PLOS ONE* 13, e0192621.
- [10] Okami, K. Clinical features and treatment strategy for HPV-related oropharyngeal cancer. *International Journal of Clinical Oncology* 21, 827–835.
- [11] Fakhry, C. *et al.* Improved Survival of Patients With Human Papillomavirus-Positive Head and Neck Squamous Cell Carcinoma in a Prospective Clinical Trial. *JNCI: Journal of the National Cancer Institute* 100, 261–269.



- [12] Hajek, M. *et al.* TRAF3/CYLD mutations identify a distinct subset of human papillomavirus-associated head and neck squamous cell carcinoma. *Cancer* 123, 1778–1790.
- [13] Oganessian, G. *et al.* Critical role of TRAF3 in the Toll-like receptor-dependent and -independent antiviral response. *Nature* 439, 208.
- [14] Annunziata, C. M. *et al.* Frequent Engagement of the Classical and Alternative NF- $\kappa$ B Pathways by Diverse Genetic Abnormalities in Multiple Myeloma. *Cancer Cell* 12, 115–130.
- [15] Chung, G. T. *et al.* Identification of a recurrent transforming UBR5–ZNF423 fusion gene in EBV-associated nasopharyngeal carcinoma. *The Journal of Pathology* 231, 158–167.
- [16] Keats, J. J. *et al.* Promiscuous Mutations Activate the Noncanonical NF- $\kappa$ B Pathway in Multiple Myeloma. *Cancer Cell* 12, 131–144.
- [17] Lechner, M. *et al.* Targeted next-generation sequencing of head and neck squamous cell carcinoma identifies novel genetic alterations in HPV+ and HPV- tumors. *Genome Medicine* 5, 49.
- [18] Parfenov, M. *et al.* Characterization of HPV and host genome interactions in primary head and neck cancers. *Proceedings of the National Academy of Sciences* 111, 15544–15549.
- [19] Walter, V. *et al.* Molecular Subtypes in Head and Neck Cancer Exhibit Distinct Patterns of Chromosomal Gain and Loss of Canonical Cancer Genes. *PLoS ONE* 8, e56823.
- [20] Marur, S., D’Souza, G., Westra, W. H. & Forastiere, A. A. HPV-associated head and neck cancer: a virus-related cancer epidemic. *The Lancet Oncology* 11, 781–789.
- [21] Moody, C. A. & Laimins, L. A. Human papillomavirus oncoproteins: pathways to transformation. *Nature Reviews Cancer* 10, 550.
- [22] Hausen, H. z. Papillomaviruses in the causation of human cancers — a brief historical account. *Virology* 384, 260–265.
- [23] Rigoni-Stern, D. Fatti statistici relativi alle malattie cancerose. *Giorn Prog Patol Terap* 2.
- [24] Strauss, M. J., Shaw, E. W., Bunting, H. & Melnick, J. L. “Crystalline” Virus-Like Particles from Skin Papillomas Characterized by Intranuclear Inclusion Bodies. *Proceedings of the Society for Experimental Biology and Medicine* 72, 46–50.
- [25] Syrjänen, S. & Syrjänen, K. The history of papillomavirus research. *Central European journal of public health* 16 Suppl, S7–13.

- [26] Rous, P. & Beard, J. W. Carcinomatous Changes in Virus-induced Papillomas of the Skin of the Rabbit. *Proceedings of the Society for Experimental Biology and Medicine* 32, 578–580.
- [27] Rous, P. & Friedewald, W. F. THE EFFECT OF CHEMICAL CARCINOGENS ON VIRUS-INDUCED RABBIT PAPILLOMAS. *The Journal of Experimental Medicine* 79, 511–538.
- [28] Rous, P. & Kidd, J. G. THE CARCINOGENIC EFFECT OF A PAPILLOMA VIRUS ON THE TARRED SKIN OF RABBITS I. DESCRIPTION OF THE PHENOMENON. *The Journal of Experimental Medicine* 67, 399–428.
- [29] Gissmann, L. *et al.* Human papillomavirus types 6 and 11 DNA sequences in genital and laryngeal papillomas and in some cervical cancers. *Proceedings of the National Academy of Sciences* 80, 560–563.
- [30] Hausen, H. z. Current Topics in Microbiology and Immunology 78, 1–30.
- [31] Hausen, H. z. Papillomaviruses and cancer: from basic studies to clinical application. *Nature Reviews Cancer* 2, nrc798.
- [32] Hebner, C. M. & Laimins, L. A. Human papillomaviruses: basic mechanisms of pathogenesis and oncogenicity. *Reviews in Medical Virology* 16, 83–97.
- [33] Koutsky, L., PhD. Epidemiology of Genital Human Papillomavirus Infection. *The American Journal of Medicine* 102, 3–8.
- [34] HPV and Cancer. URL [https://www.cdc.gov/cancer/hpv/basic\\_info/hpv\\_oropharyngeal.htm](https://www.cdc.gov/cancer/hpv/basic_info/hpv_oropharyngeal.htm).
- [35] Lehoux, M., D'Abramo, C. M. & Archambault, J. Molecular Mechanisms of Human Papillomavirus-Induced Carcinogenesis. *Public Health Genomics* 12, 268–280.
- [36] Lydiatt, W. M. *et al.* Head and Neck cancers—major changes in the American Joint Committee on cancer eighth edition cancer staging manual. *CA: A Cancer Journal for Clinicians* 67, 122–137.
- [37] Baltimore, D. Discovering NF- $\kappa$ B. *Cold Spring Harbor Perspectives in Biology* 1, a000026.
- [38] Celebrating 25 years of NF- $\kappa$ B. *Nature Immunology* 12, 681.
- [39] Sen, R. The origins of NF- $\kappa$ B. *Nature Immunology* 12, 686.
- [40] Oeckinghaus, A., Hayden, M. S. & Ghosh, S. Crosstalk in NF- $\kappa$ B signaling pathways. *Nature Immunology* 12, 695.
- [41] Zarnegar, B. J. *et al.* Noncanonical NF- $\kappa$ B activation requires coordinated assembly of a regulatory complex of the adaptors cIAP1, cIAP2, TRAF2 and TRAF3 and the kinase NIK. *Nature Immunology* 9, 1371–1378.

- [42] Hershko, A. & Ciechanover, A. THE UBIQUITIN SYSTEM. *Annual Review of Biochemistry* 67, 425–479.
- [43] Ciechanover, A. The ubiquitin–proteasome proteolytic pathway. *Cell* 79, 13–21.
- [44] Ohtake, F., Saeki, Y., Ishido, S., Kanno, J. & Tanaka, K. The K48–K63 Branched Ubiquitin Chain Regulates NF- $\kappa$ B Signaling. *Molecular cell* 64, 251–266.
- [45] Vallabhapurapu, S. *et al.* Nonredundant and complementary functions of TRAF2 and TRAF3 in a ubiquitination cascade that activates NIK-dependent alternative NF- $\kappa$ B signaling. *Nature Immunology* 9, ni.1678.
- [46] Häcker, H., Tseng, P.-H. & Karin, M. Expanding TRAF function: TRAF3 as a tri-faced immune regulator. *Nature Reviews Immunology* 11, 457.
- [47] Bignell, G. R. *et al.* Identification of the familial cylindromatosis tumour-suppressor gene. *Nature Genetics* 25, nsg0600,60.
- [48] Kovalenko, A. *et al.* The tumour suppressor CYLD negatively regulates NF- $\kappa$ B signalling by deubiquitination. *Nature* 424, 801.
- [49] Sun, S.-C. CYLD: a tumor suppressor deubiquitinase regulating NF- $\kappa$ B activation and diverse biological processes. *Cell Death and Differentiation* 17, cdd200943.
- [50] Brummelkamp, T. R., Nijman, S. M. B., Dirac, A. M. G. & Bernards, R. Loss of the cylindromatosis tumour suppressor inhibits apoptosis by activating NF- $\kappa$ B. *Nature* 424, 797.
- [51] Baldwin, A. S. Series Introduction: The transcription factor NF- $\kappa$ B and human disease. *Journal of Clinical Investigation* 107, 3–6.
- [52] Geimanen, J. *et al.* Development of a Cellular Assay System To Study the Genome Replication of High- and Low-Risk Mucosal and Cutaneous Human Papillomaviruses. *Journal of Virology* 85, 3315–3329.
- [53] Isok-Paas, H., Männik, A., Ustav, E. & Ustav, M. The transcription map of HPV11 in U2OS cells adequately reflects the initial and stable replication phases of the viral genome. *Virology Journal* 12, 59.
- [54] Orav, M. *et al.* Recombination-Dependent Oligomerization of Human Papillomavirus Genomes upon Transient DNA Replication. *Journal of Virology* 87, 12051–12068.
- [55] Toots, M. *et al.* Identification of several high-risk HPV inhibitors and drug targets with a novel high-throughput screening assay. *PLOS Pathogens* 13, e1006168.
- [56] Ang, K. K. *et al.* Human Papillomavirus and Survival of Patients with Oropharyngeal Cancer. *The New England Journal of Medicine* 363, 24–35.
- [57] Corry, J., Peters, L. J. & Rischin, D. Optimising the therapeutic ratio in head and neck cancer. *The Lancet Oncology* 11, 287–291.

- [58] Masterson, L. *et al.* De-escalation treatment protocols for human papillomavirus-associated oropharyngeal squamous cell carcinoma: A systematic review and meta-analysis of current clinical trials. *European Journal of Cancer* 50, 2636–2648.
- [59] Spence, T., Bruce, J., Yip, K. W. & Liu, F.-F. HPV Associated Head and Neck Cancer. *Cancers* 8, 75.
- [60] Sano, D. & Oridate, N. The molecular mechanism of human papillomavirus-induced carcinogenesis in head and neck squamous cell carcinoma. *International Journal of Clinical Oncology* 21, 819–826.
- [61] Ben-Neriah, Y. & Karin, M. Inflammation meets cancer, with NF- $\kappa$ B as the matchmaker. *Nature Immunology* 12, 715.
- [62] Taniguchi, K. & Karin, M. NF- $\kappa$ B, inflammation, immunity and cancer: coming of age. *Nature Reviews Immunology* 18, 309.
- [63] Marur, S. *et al.* E1308: Phase II Trial of Induction Chemotherapy Followed by Reduced-Dose Radiation and Weekly Cetuximab in Patients With HPV-Associated Resectable Squamous Cell Carcinoma of the Oropharynx— ECOG-ACRIN Cancer Research Group. *Journal of Clinical Oncology* 35, 490–497.
- [64] Hutchin, M., Pickles, R. & Yarbrough, W. Efficiency of adenovirus-mediated gene transfer to oropharyngeal epithelial cells correlates with cellular differentiation and human coxsackie and adenovirus receptor .... *Human gene therapy* .
- [65] Shores, C. G. & Yarbrough, W. G. Three-dimensional xenograft model of dysplastic human laryngeal mucosa. *The Laryngoscope* 108, 1358–1362.